Thermodynamics of transport through the ammonium transporter Amt-1 investigated with free energy calculations

R. Thomas Ullmann*,†, Susana L. A. Andrade‡ and G. Matthias Ullmann*,†

† Structural Biology / Bioinformatics, University of Bayreuth, Universitätsstr. 30, BGI, 95447 Bayreuth, Germany

‡ Lehrstuhl für Biochemie, Institut für organische Chemie und Biochemie, Albert-Ludwigs-Universität Freiburg, Albertstrasse 21, 79104 Freiburg, Germany.

∗ Email: thomas.ullmann@uni-bayreuth.de; matthias.ullmann@uni-bayreuth.de

Supporting Information

Contents

intracellular side		extracellular side
Tyr-27	Lys-293	Asp-3
Arg-32	Lys-294	Tyr-57
Arg-33	Asp-296	Tyr-59
Lys-34	Glu-297	Asp-66
Glu-110	Asp-300	Tyr-76
Arg-111	His-305	Lys-83
Lys-113	Lys-361	Glu-85
His-157	Asp-364	Asp-86
Lys-173	Arg-370	Tyr-92
Arg-174	Glu-375	Tyr-129
Glu-178	Glu-376	His-134
Glu-179	Tyr-377	Lys-144
Tyr-180	Asp-381	Asp-149
Glu-183	His-385	Asp-214
His-185	Glu-386	Asp-268
Lys-241	Glu-387	Lys-270
Lys-243	Tyr-390	Glu-323
Cys-283	Am2	Tyr-327
Tyr-284	Am3	Tyr-351
Asp-288	Am4	Am1a
Arg-290	Am5	Am1b
Lys-292	Am6	

Table S1: Titratable sites connected to the intracellular and extracellular sides.

A Parameters

This section specifies the parameters used in our calculations.

Connectivities of the sites to the membrane sides

The connectivities of each site to either solvent phase are listed in Table S1.

Atomic partial charges

The permeant species are represented with tetrahedral models similar to 5-site water models commonly used in molecular dynamics (see main text). Table S2 lists the atomic partial charges of the binding forms of the permeant sites. The atomic partial charges of non-standard forms of amino acid side chains not available from the CHARMM22 parameter set [1] are listed in the Supporting Information of reference 2.

Intrinsic model energies

Table S3 lists the model energies of the microscopic forms of the permeant sites in Amt-1. The microscopic intrinsic energies are calculated as described in the main text using the standard chemical potentials of the macroscopic protonation forms listed in Table S4. The model energies of all other residues are listed in the Supporting Information of reference 2.

The intrinsic model energies of the permeant sites are derived as follows. The intrinsic model energy of an instance k of a site i is given by

$$E_{i,k}^{\mathrm{int,r}} = \mu_{i,k}^{\circ} - \mu^{\circ,\mathrm{ref}} \tag{S1}$$

where $\mu_{i,k}^{\circ}$ is the standard chemical potential of the model compound for the site in the corresponding form. The ligand-free form of the site is chosen as reference form so that $\mu^{\circ,\mathrm{ref}} = 0$ kcal/mol.

Our model considers multiple microscopic forms for each permeant species to model different orientations of the permeant in the binding site. The intrinsic model energy of a microscopic binding form

has to be corrected for the number of rotamers x included for the permeant species to retain the correct statistical weight relative to other permeant species[3,4]

$$E_{i,k}^{\mathrm{int,r}} = E_{i,k}^{\mathrm{int,macro}} + \beta^{-1} \ln [x] - \frac{2}{2}\beta^{-1} \tag{S2}$$

where we exploited the equivalence of the rotamers in the isotropic solvent environment. The additional term of $-\frac{2}{2}\beta^{-1}$ accounts for the kinetic energy liberated upon the loss of two translational degrees of freedom when the permeant is transferred from the solution to the transmembrane pore. In the solvent, the permeant can diffuse freely in three dimensions whereas in the transmembrane pore the permeant is essentially restricted to one dimensional diffusion normal to the membrane plane.

A possible loss of translational entropy accompanying the transfer from the solution to the transmembrane pore is difficult to quantify with certainty. The corresponding free energy contribution is likely very small because the permeants are already tightly packed in the solvent environment[5]. Therefore, we did not include such a contribution in the intrinsic model energies.

Confidence in our binding model can be gained through a small Gedankenexperiment. The removal of a water molecule from the bulk solvent to create an apolar cavity has a free energy cost of 2.4 kcal/mol. This value compares favorably to the experimental solvation free energy of 1.94 to 2.0 kcal/mol for the apolar molecule methane which has a similar size as ammonia or water[6,7]. Theoretical values for the solvation free energy of methane compare even better to our result (2.2 kcal/mol[8], 2.4 to 2.5 kcal/mol[9,10]).

The permeant species were modeled as regular tetrahedra with five interaction centers placed at the center and the corners of the tetrahedra. This representation permits a very efficient treatment of rotameric forms for the permeant sites and has already proven useful in our recent study of the proton transfer through gramicidin[11]. The central oxygen or nitrogen atom of the permeants are placed at the center of the tetrahedron. Each corner of the tetrahedron is occupied by a hydrogen atom or a lone electron pair. The distance between the center and the peripheral interaction centers of the water and ammonia models is 0.9526 Å and 1.0272 Å, respectively. Rotamers are obtained from the different possible permutations for the distribution of the hydrogen atoms and the lone electron pairs to the corners of the tetrahedra. Additional rotamers were added for all permeant sites by randomly rotating the initially generated coordinates in space resulting in an eightfold increase in the number of rotamers.

B Expressions for the description of binding equilibria in terms of chemical potentials

This section lists some equations needed to describe the binding equilibria of model compounds in terms of experimentally determined chemical potentials. These derivations resulted in the expressions for the activities of the permeants used in the main paper. We show how to derive expressions for the equilibrium population of macroscopic receptor species within a chemical potential based formulation of binding equilibria. The partition function is obtained as central quantity of the binding thermodynamics. It is shown that the appearance of the partition function in the formalism is a consequence of imposing the equilibrium conditions.

The binding equilibrium of a monovalent receptor can be described by

$$\mathrm{R} + \mathrm{L} \overset{K_\mathrm{a}}{\rightleftharpoons} \mathrm{RL} \tag{S3}$$

where K_a is the association constant. The chemical potential of a chemical species i in solution is defined as

$$\mu_i = \mu_i^\circ + \beta^{-1} \ln a_i \tag{S4}$$

where μ_i° is the standard chemical potential of the species in solution corresponding to its standard concentration c_i°. The activity a_i of a species i can be defined on the basis of the actual and standard concentrations as

$$a_i = \gamma_i \frac{c_\mathrm{i}}{c_\mathrm{i}^\circ} \tag{S5}$$

The activity coefficient γ_i accounts for interactions between compounds within the system that are not otherwise accounted for by the model and thus lead to deviations from an ideal behavior. Here, ideal

Atom	Charge in $e_\circ$
NH_3	
N	-0.195355
H1	0.124037
H2	0.124037
H3	0.124037
LP	-0.176756
NH_4^+	
N	-0.442588
H1	0.360647
H2	0.360647
H3	0.360647
H4	0.360647
OH^-	
O	-0.730332
H1	0.001088
LP1	-0.090252
LP2	-0.090252
LP3	-0.090252
H_2O	
O	-0.221816
H1	0.223871
H2	0.223871
LP1	-0.107173
LP2	-0.107173
H_3O^+	
O	0.108985
H1	0.326498
H2	0.326498
H3	0.326498
LP1	-0.088479

Table S2: Atomic partial charges for the binding forms of the channel sites. Only one rotameric form is given for each bound species. Charges of chemically equivalent atoms were averaged. The form label empty denotes that the site is unoccupied. Atom names beginning with N, O, H or LP correspond to the nitrogen atoms, oxygen atoms, hydrogen atoms and lone electron pairs, respectively.

Microscopic form	$\mu^{\circ,\mathrm{macro}}$ in kcal/mol	number of microscopic forms	Intrinsic energy in kcal/mol
empty	0.00	1	0.00
occupied by NH_3	-6.35	4	-6.12
occupied by NH_4^+	-18.97	1	-19.56
occupied by OH^-	-37.59	4	37.36
occupied by H_2O	-56.69	6	-56.22
occupied by H_3O^+	-54.37	4	-54.14

Table S3: Intrinsic model energies for model compounds of the permeant binding sites in Amt-1. The permeant binding sites can be unoccupied, occupied by a protonation form of water or occupied by a protonation form of ammonia. The protonation forms of ammonia and water are represented by tetrahedral models (see text). All $\mathrm{p}K_\mathrm{a}^\mathrm{macro}$ values measured in water. All model energies referenced to water. Values for $\mu^{\circ,\mathrm{macro}}$ were taken from Table S4. The microscopic model chemical potential is given by $\mu^{\circ,\mathrm{micro}} = \mu^{\circ,\mathrm{macro}} + \beta^{-1}\ln[n]$ where n is the number of microscopic forms representing the species. In bulk solution, the permeant possesses three translational degrees of freedom along all spatial dimensions. Within the transmembrane pore, the movement of the permeant is essentially restricted to a one dimensional translation along the membrane pore. Thus, the transfer of the permeant from the solution to the transmembrane pore leads to an effective loss of two translational degrees of freedom. An additional term $-\frac{2}{2}\beta^{-1}$ is added to the intrinsic model energy of non-empty forms to account for the corresponding amount of kinetic energy thus liberated.

behavior would mean that the chemical potential of the compound is strictly linearly dependent on the compound concentration, that is $\gamma_i = 1$. In general, the activity coefficient is concentration dependent. In dilute solution, the activity coefficient can be assumed to be concentration independent over a wide range of concentrations. The interactions between the compounds of a mixture may be divided into nonspecific interactions and specific interactions. Specific interactions can for example comprise the binding of different compounds to form a new compound. Such bound compound species can also be considered explicitly as will be shown below for ligands with multiple protonation forms. Nonspecific interactions in aqueous solution are dominated by the nonspecific electrostatic interactions of a compound with mobile ions. These interactions can for example be modeled with continuum electrostatics theory in different mathematical realizations of varying complexity. A simple mathematical realization of the continuum electrostatics model that can be used to model these interactions for ions that are reasonably approximated by a spherical shape is the Debye-Hückel equation[12–14]. The standard state can be chosen such that all significant nonspecific interactions of the compound are included in the standard chemical potential. If, in addition, all relevant bound species are modeled explicitly, the value of the activity coefficients will approach 1. In this limit, which we might term the limit of a complete model, the activity can be approximated by the ratio of the corresponding concentration and the standard concentration

$$a_i \approx \frac{c_i}{c^\circ} \tag{S6}$$

In the presence of an electrostatic potential, an additional term is needed to account for the interaction energy of the charge of the species with the electrostatic potential. The resulting electrochemical potential $\bar{\mu}$ is often written with a bar to distinguish it from the purely chemical potential μ

$$\bar{\mu}_i = \mu_i + z_i \mathrm{F} \phi \tag{S7}$$

where z_i is the formal charge of the species and ϕ is the electrostatic potential at the spatial position of the species. The sum of the last term in Eq. (S7) for all species taking part in a reaction will not change if the reaction takes place within a phase with a uniform electrostatic potential, because the total charge (monopole of the charge distribution) is always conserved. The electrostatic contribution to reaction free energies can be non-vanishing, if the electrostatic potential is not uniform throughout the whole phase, that is if its gradient (the electric field) does not vanish everywhere. This is, because the dipole and the higher moments of the charge distribution can change during a reaction, which can lead to a change of their potential energy in the electric field. The electrostatic contribution to a reaction free energy can also not be neglected if chemical species from different phases of differing electrostatic potential take part in the reaction. An example for such a reaction would be the transport of a charged species across a membrane with a transmembrane electrostatic potentials gradient as (see Sec. C).

The sum of the changes in the standard chemical potential and the activity coefficient dependent chemical potential terms of the receptor species upon binding can be termed the intrinsic standard binding free energy

$$G^{\mathrm{int}} = \mu^\circ_{\mathrm{RL}} - \mu^\circ_{\mathrm{R}} + \beta^{-1} \ln \left[\frac{\gamma_{\mathrm{RL}}}{\gamma_{\mathrm{R}}} \right] \tag{S8}$$

The difference in the standard chemical potentials of the products and reactants of the binding reaction is equal to the standard binding free energy

$$G^{\mathrm{bind},\circ} = G^{\mathrm{int}} - \mu^\circ_L \tag{S9}$$

which is given by

$$\begin{aligned} G^{\mathrm{bind},\circ} &= -\beta^{-1} \ln K^\circ_a \\ &= -\beta^{-1} \ln \left[\frac{c_{\mathrm{RL}}}{c_{\mathrm{R}} c^\circ_{\mathrm{L}}} \frac{\gamma_{\mathrm{RL}}}{\gamma_{\mathrm{R}}} \right] \quad \text{with} \quad c_{\mathrm{R}} + c_{\mathrm{RL}} = c^\circ \end{aligned} \tag{S10}$$

where c° is the standard concentration, usually defined as $c^\circ = 1\,\mathrm{M}$. The activity coefficient dependent terms and factors in Eqs. (S8), (S9) and (S10) can be omitted under the conditions described above where all activity coefficients approach unity. The binding free energy at arbitrary concentrations of

ligand and receptor is given by the difference of the summed chemical potentials of the products and reactants occurring in the binding reaction

$$G^{\mathrm{bind}} = G^{\mathrm{int}} - \mu_{\mathrm{L}} \tag{S11}$$

If the ligand is the proton, the ligand chemical potential is given by

$$\mu_{\mathrm{L}} = -\beta^{-1} \ln(10)\, \mathrm{pH} \tag{S12}$$

where $a_{\mathrm{H^+}} \equiv 10^{-\mathrm{pH}}$ [15] and ($\mu^{\circ}_{\mathrm{H^+}} \equiv 0$ by definition). If the receptor is a monoprotic acid, the intrinsic energies and binding free energies can be expressed in terms of its $\mathrm{p}K_{\mathrm{a}} = -\log_{10} K_{\mathrm{a}}$ and the chemical potential of the proton. The intrinsic energy, defined by Eq. (S10), of a monoprotic acid is given by

$$G^{\mathrm{int}} = -\beta^{-1} \ln 10\ \mathrm{p}K_{\mathrm{a}} \tag{S13}$$

Consequently, the protonation free energy is given by

$$G^{\mathrm{bind}} = -\beta^{-1} \ln 10\ \ (\mathrm{p}K_{\mathrm{a}} - \mathrm{pH}) \tag{S14}$$

In the following sections, we derive the expressions for the activities of the permeants used in the main paper. For the derivations, we assume that the model is complete as described above. That is, we assume that all nonspecific interactions are accounted for by the standard chemical potentials and that all specific interactions are explicitly considered in the model by including all relevant binding forms of the permeants. In this limit, all activity coefficients are equal to one, and we can express the activity of a species i in terms of concentration and standard concentration only $a_i = \frac{c_i}{c^{\circ}}$. A general derivation that accounts for arbitrary binding reactions and activity coefficients that deviate from a value of one will be presented elsewhere. This derivation ultimately leads to the binding formalism utilized in our software suite GMCT[4]. Some more detail about the calculation of intrinsic model energies from experimental data can be found in reference 4.

B.1 The binding equilibrium for a monovalent receptor

In an experimental setup, one will usually know the total concentration of the bound and unbound receptor molecules added to the solution and the concentration of the ligand. The reaction scheme for the binding reaction is

$$\mathrm{R} + \mathrm{L} \overset{K_{\mathrm{a}}}{\rightleftharpoons} \mathrm{RL} \tag{S15}$$

Under the above mentioned conditions, we can assume that all activity coefficients are equal to one and the chemical potential of each compound species i is given by

$$\mu_{\mathrm{i}} = \mu^{\circ}_i + \beta^{-1} \ln \frac{c_i}{c^{\circ}_i} \tag{S16}$$

In equilibrium the sum of the chemical potentials of the products is equal to that of the reactants, providing us with a basis for an expression relating the chemical potential of the bound and unbound receptor species to the total receptor concentration and the ligand concentration

$$\sum_{i}^{\text{reactants}} \mu_i = \sum_{j}^{\text{products}} \mu_j \tag{S17}$$

Using the reaction scheme Eq. (S15) and the expression for the chemical potential of a species Eq. (S16) we obtain

$$\begin{aligned} \mu_{\mathrm{R}} + \mu_{\mathrm{L}} &= \mu_{\mathrm{RL}} \\ \mu_{\mathrm{R}} &= \mu_{\mathrm{RL}} - \mu_{\mathrm{L}} \end{aligned} \tag{S18}$$

Inserting the expression for the chemical potentials of each species according to Eq. (S16) into Eq. (S18) yields

$$\mu^{\circ}_{\mathrm{R}} + \beta^{-1} \ln a_{\mathrm{R}} = \mu^{\circ}_{\mathrm{RL}} + \beta^{-1} \ln a_{\mathrm{RL}} - \mu^{\circ}_{\mathrm{L}} - \beta^{-1} \ln a_{\mathrm{L}} \tag{S19}$$

which can be rearranged to obtain an expression for a_{R}

$$\beta^{-1} \ln a_{\mathrm{R}} = \mu^{\circ}_{\mathrm{RL}} - \mu^{\circ}_{\mathrm{R}} - \mu^{\circ}_{\mathrm{L}} + \beta^{-1} \ln a_{\mathrm{RL}} - \beta^{-1} \ln a_{\mathrm{L}} \tag{S20}$$

Assuming that the activity coefficients of all receptor species are unity and that all standard concentrations are identical, we can write the total activity of all receptor species a sum over the individual activities expressed in terms of the concentrations

$$\begin{aligned} a_{\mathrm{RX}} &= a_{\mathrm{R}} + a_{\mathrm{RL}} \\ &= \frac{c_{\mathrm{R}} + c_{\mathrm{RL}}}{c^{\circ}} \end{aligned} \tag{S21}$$

From Eq. (S21), we can write

$$a_{\mathrm{RL}} = a_{\mathrm{RX}} - a_{\mathrm{R}} \tag{S22}$$

This expression is inserted into Eq. (S20) to obtain

$$\beta^{-1} \ln \frac{a_{\mathrm{R}}}{a_{\mathrm{RX}} - a_{\mathrm{R}}} = \mu^{\circ}_{\mathrm{RL}} - \mu^{\circ}_{\mathrm{R}} - \mu^{\circ}_{\mathrm{L}} - \beta^{-1} \ln a_{\mathrm{L}} \tag{S23}$$

The first two terms on the right-hand side can be recognized as the intrinsic energy E_1^{int} of the occupied receptor with the empty receptor chosen as reference state (see Eq. (S8)), whereas the last two terms constitute the ligand chemical potential μ_{L}. We rewrite Eq. (S23) in terms of these quantities and solve for a_{R}

$$\frac{a_{\mathrm{R}}}{a_{\mathrm{RX}} - a_{\mathrm{R}}} = \exp\left[\beta \left(E_1^{\mathrm{int}} - \mu_{\mathrm{L}}\right)\right] \tag{S24}$$

$$a_{\mathrm{RX}} = a_{\mathrm{R}} \left(1 + \exp\left[-\beta \left(E_1^{\mathrm{int}} - \mu_{\mathrm{L}}\right)\right]\right) \tag{S25}$$

$$a_{\mathrm{R}} = a_{\mathrm{RX}} \frac{1}{1 + \exp\left[-\beta \left(E_1^{\mathrm{int}} - \mu_{\mathrm{L}}\right)\right]} \tag{S26}$$

The latter expression for the activity of the unbound receptor species can be written as

$$a_{\mathrm{R}} = a_{\mathrm{RX}} \left(1 - \langle x \rangle\right) \tag{S27}$$

where $\langle x \rangle = 1/\exp\left[-\beta \left(E_1^{\mathrm{int}} - \mu_{\mathrm{L}}\right)\right]$ is the equilibrium binding probability. The corresponding equation for the activity of the bound receptor species can be obtained using Eq. (S21) as

$$a_{\mathrm{RL}} = a_{\mathrm{RX}} \langle x \rangle \tag{S28}$$

which gives combined with Eq. (S26)

$$a_{\mathrm{RL}} = a_{\mathrm{RX}} \frac{\exp\left[-\beta \left(E_1^{\mathrm{int}} - \mu_{\mathrm{L}}\right)\right]}{1 + \exp\left[-\beta \left(E_1^{\mathrm{int}} - \mu_{\mathrm{L}}\right)\right]} \tag{S29}$$

The term in the denominator of the fraction in Eqs. (S26) and (S29) can be recognized as the partition function $\mathcal{Z}$ of the receptor-ligand system

$$\mathcal{Z} = 1 + \exp\left[-\beta \left(E_1^{\mathrm{int}} - \mu_{\mathrm{L}}\right)\right] \tag{S30}$$

The 1 on the right-hand side of Eq. (S30) is the Boltzmann weight of the empty receptor, $\exp\left[-\beta E_0^{\mathrm{int}}\right] = 1$, where $E_0^{\mathrm{int}} = 0$. The intrinsic energy of the empty receptor is equal to zero according to Eq. (S8), because we chose the empty receptor species as reference form.

B.2 The binding equilibrium for a divalent receptor

The derivation of the equilibrium chemical potentials of the binding forms for a divalent receptor follows the same route as that for the monovalent receptor. Again, the ligand concentration, and the total concentration of the receptor species are known. Here, we adopt a macroscopic view, i.e., we distinguish the receptor species based on the total number of ligands bound. The reaction scheme showing the two binding steps is

$$\mathrm{R} + 2\,\mathrm{L} \overset{K_{\mathrm{a},1}}{\rightleftharpoons} \mathrm{RL} + \mathrm{L} \overset{K_{\mathrm{a},2}}{\rightleftharpoons} \mathrm{RL}_2 \tag{S31}$$

The sum of the chemical potentials of all species is equal for each stage of the reaction scheme which leads to two equations relating the equilibrium chemical potentials of all the receptor species to each other. Using the reaction scheme Eq. (S31) and the expression for the chemical potential of a species Eq. (S16) we obtain

$$\begin{aligned} \mu_{\mathrm{R}} + \mu_{\mathrm{L}} &= \mu_{\mathrm{RL}} \\ \mu_{\mathrm{R}} &= \mu_{\mathrm{RL}} - \mu_{\mathrm{L}} \end{aligned} \tag{S32}$$

and

$$\begin{aligned} \mu_{\mathrm{RL}} + \mu_{\mathrm{L}} &= \mu_{\mathrm{RL}_2} \\ \mu_{\mathrm{RL}} &= \mu_{\mathrm{RL}_2} - \mu_{\mathrm{L}} \end{aligned} \tag{S33}$$

Substitution of Eq. (S33) for μ_{RL} in Eq. (S32) gives

$$\mu_{\mathrm{R}} = \mu_{\mathrm{RL}_2} - 2\mu_{\mathrm{L}} \tag{S34}$$

Inserting the expression for the chemical potentials of each species according to Eq. (S16) into Eq. (S34) yields

$$\mu^{\circ}_{\mathrm{R}} + \beta^{-1} \ln a_{\mathrm{R}} = \mu^{\circ}_{\mathrm{RL}_2} + \beta^{-1} \ln a_{\mathrm{RL}_2} - 2\mu^{\circ}_{\mathrm{L}} - 2\beta^{-1} \ln a_{\mathrm{L}} \tag{S35}$$

which can be rearranged to obtain an expression for a_{R}

$$\beta^{-1} \ln a_{\mathrm{R}} = +\beta^{-1} \ln a_{\mathrm{RL}_2} + \mu^{\circ}_{\mathrm{RL}_2} - \mu^{\circ}_{\mathrm{R}} - 2\mu^{\circ}_{\mathrm{L}} - 2\beta^{-1} \ln a_{\mathrm{L}} \tag{S36}$$

Assuming that all activity coefficients are unity and all standard concentrations are identical, we can write the total activity of all receptor species a sum over the individual activities expressed in terms of the concentrations

$$\begin{aligned} a_{\mathrm{RX}} &= a_{\mathrm{R}} + a_{\mathrm{RL}} + a_{\mathrm{RL}_2} \\ &= \frac{c_{\mathrm{R}} + c_{\mathrm{RL}} + c_{\mathrm{RL}_2}}{c^{\circ}} \end{aligned} \tag{S37}$$

from which we can write

$$a_{\mathrm{RL}_2} = a_{\mathrm{RX}} - a_{\mathrm{R}} - a_{\mathrm{RL}} \tag{S38}$$

This expression is inserted into Eq. (S36) to obtain

$$\beta^{-1} \ln \frac{a_{\mathrm{R}}}{a_{\mathrm{RX}} - a_{\mathrm{R}} - a_{\mathrm{RL}}} = \mu^{\circ}_{\mathrm{RL}_2} - \mu^{\circ}_{\mathrm{R}} - 2\mu^{\circ}_{\mathrm{L}} - 2\beta^{-1} \ln a_{\mathrm{L}} \tag{S39}$$

The first two terms on the right-hand side can be recognized as the the intrinsic energy of the doubly occupied receptor

$$E_2^{\mathrm{int}} = \mu^{\circ}_{\mathrm{RL}_2} - \mu^{\circ}_{\mathrm{R}} \tag{S40}$$

according to Eq. (S8), whereas the last two terms constitute twice the ligand chemical potential μ_{L}. We rewrite Eq. (S39) in terms of these quantities and solve for a_{R}

$$\frac{a_{\mathrm{R}}}{a_{\mathrm{RX}} - a_{\mathrm{R}} - a_{\mathrm{RL}}} = \exp\left[\beta\left(E_2^{\mathrm{int}} - 2\mu_{\mathrm{L}}\right)\right] \tag{S41}$$

$$\frac{a_{\mathrm{RX}} - a_{\mathrm{R}} - a_{\mathrm{RL}}}{a_{\mathrm{R}}} = \exp\left[-\beta\left(E_2^{\mathrm{int}} - 2\mu_{\mathrm{L}}\right)\right] \tag{S42}$$

$$a_{\mathrm{RX}} - a_{\mathrm{R}} - a_{\mathrm{RL}} = a_{\mathrm{R}} \exp\left[-\beta\left(E_2^{\mathrm{int}} - 2\mu_{\mathrm{L}}\right)\right] \tag{S43}$$

$$a_{\mathrm{RX}} - a_{\mathrm{RL}} = a_{\mathrm{R}}\left(1 + \exp\left[-\beta\left(E_2^{\mathrm{int}} - 2\mu_{\mathrm{L}}\right)\right]\right) \tag{S44}$$

Here, we still need to eliminate a_{RL}. For this purpose, we rearrange Eq. (S32) using Eq. (S16) for the chemical potentials of the receptor species

$$\begin{aligned} \mu_{\mathrm{RL}} &= \mu_{\mathrm{R}} + \mu_{\mathrm{L}} && \text{(S45)} \\ \mu^{\circ}_{\mathrm{RL}} + \beta^{-1} \ln a_{\mathrm{RL}} &= \mu^{\circ}_{\mathrm{R}} + \beta^{-1} \ln a_{\mathrm{R}} + \mu^{\circ}_{\mathrm{L}} + \beta^{-1} \ln a_{\mathrm{L}} && \text{(S46)} \\ \beta^{-1} \ln \frac{a_{RL}}{a_{\mathrm{R}}} &= \mu^{\circ}_{\mathrm{R}} - \mu^{\circ}_{\mathrm{RL}} + \mu_{\mathrm{L}} && \text{(S47)} \end{aligned}$$

where we recognize the intrinsic energy of the singly occupied receptor species $E_1^{\mathrm{int}} = \mu^{\circ}_{\mathrm{RL}} - \mu^{\circ}_{\mathrm{R}}$ and solve for a_{RL}

$$a_{RL} = a_R \exp\left[-\beta\left(E_1^{\mathrm{int}} - \mu_{\mathrm{L}}\right)\right] \tag{S48}$$

This expression is inserted into Eq. (S44) to obtain a_{R}

$$a_{\mathrm{R}} = a_{\mathrm{RX}} \frac{1}{1 + \exp\left[-\beta\left(E_1^{\mathrm{int}} - \mu_{\mathrm{L}}\right)\right] + \exp\left[-\beta\left(E_2^{\mathrm{int}} - 2\mu_{\mathrm{L}}\right)\right]} \tag{S49}$$

The activity of the species RL is obtained by inserting Eq. (S49) into Eq. (S44)

$$a_{\mathrm{RL}} = a_{\mathrm{RX}} \frac{\exp\left[-\beta\left(E_1^{\mathrm{int}} - \mu_{\mathrm{L}}\right)\right]}{1 + \exp\left[-\beta\left(E_1^{\mathrm{int}} - \mu_{\mathrm{L}}\right)\right] + \exp\left[-\beta\left(E_2^{\mathrm{int}} - 2\mu_{\mathrm{L}}\right)\right]} \tag{S50}$$

Finally, the activity of the fully bound receptor is obtained from the latter two equations exploiting Eq. (S38)

$$a_{\mathrm{RL}_2} = a_{\mathrm{RX}} \frac{\exp\left[-\beta\left(E_2^{\mathrm{int}} - 2\mu_{\mathrm{L}}\right)\right]}{1 + \exp\left[-\beta\left(E_1^{\mathrm{int}} - \mu_{\mathrm{L}}\right)\right] + \exp\left[-\beta\left(E_2^{\mathrm{int}} - 2\mu_{\mathrm{L}}\right)\right]} \tag{S51}$$

The term in the denominator of the fraction in Eqs. (S49), (S50) and (S51) can be recognized as the partition function $\mathcal{Z}$ of the receptor-ligand system

$$\mathcal{Z} = 1 + \exp\left[-\beta\left(E_1^{\mathrm{int}} - \mu_{\mathrm{L}}\right)\right] + \exp\left[-\beta\left(E_2^{\mathrm{int}} - 2\mu_{\mathrm{L}}\right)\right] \tag{S52}$$

B.3 The binding equilibrium for an N-valent receptor

Here we consider general expressions for the macroscopic binding equilibrium of an N-valent receptor-ligand system including electrostatic potential contributions. The partition function $\mathcal{Z}$ of the receptor-ligand system in solution can formally be written as

$$\begin{aligned} \mathcal{Z} &= \sum_{n=0}^{N} \exp\left[-\beta\left(E_n^{\mathrm{int}} - n\bar{\mu}_{\mathrm{L}}\right)\right] \\ \text{with} \quad E_n^{\mathrm{int}} &= \bar{\mu}^{\circ}_{\mathrm{RL}_n} - \bar{\mu}^{\circ}_{\mathrm{RL}_0} \end{aligned} \tag{S53}$$

where N is the maximum number of bound ligands and n is the number of bound ligands in a specific macrostate. The activity of the individual receptor species is given by

$$\begin{aligned} a_{\mathrm{RL}_n} &= a_{\mathrm{tot}} \frac{\exp\left[-\beta\left(E_n^{\mathrm{int}} - n\bar{\mu}_{\mathrm{L}}\right)\right]}{Z} \\ \text{with} \quad a_{\mathrm{tot}} &= \sum_{n}^{N} \frac{c_{\mathrm{RL}_n}}{c^{\circ}} \end{aligned} \tag{S54}$$

where again the activity coefficients γ_{RL_x} of all receptor species are assumed to be unity and all standard concentrations are chosen to be equal. Then, the electrochemical potential of the species is given by

$$\bar{\mu}_{\mathrm{RL}_n} = \mu^{\circ}_{\mathrm{RL}_n} + \beta^{-1} \ln \frac{a_{\mathrm{RL}_n}}{a^{\circ}} + z_{\mathrm{RL}_n} \mathrm{e}_{\circ} \phi \tag{S55}$$

where $e_\circ$ is the elementary charge, z_i is the formal charge and the standard activity is usually chosen as $a^\circ = 1$. The electrostatic potential ϕ can contain contributions from an externally applied potential, an electrical transmembrane potential and from the electrostatic potential of other compounds in the solution.

Up to now, our formalism adopts a macroscopic view on the binding equilibria. That is, the precise microscopic configuration of the receptor is not considered. The chemical potentials stated for macroscopic binding states ($0, 1..., n$ ligands bound), contain thermodynamic averages over all possible microscopic configurations of the receptor compatible with the macroscopic binding state. If we have, for example, a rigid receptor with N sites which can either be empty or bind one ligand, then there are 2^N microscopic binding states in total, while there are $N+1$ macroscopic binding states. Already for a receptor with more than one site, there are more microscopic than macroscopic binding states. In a more realistic model, there will be often more than two forms of each site, which may differ by the number of bound ligands, the binding topology (*e.g*, tautomeric forms), the conformation (*e.g*, amino acid sidechain tautomers) or other properties. The electrochemical potential of the macroscopic binding state with n ligands bound does then involve the partition function of all microscopic receptor configurations having bound this number of ligands. If there are M microscopic receptor configurations with n ligands bound, then the electrochemical potential of the macroscopic binding state is given by

$$\bar{\mu}_{\mathrm{RL}_n} = -\beta^{-1} \ln \left[\sum_{m=1}^{M} \exp \left[-\beta \bar{\mu}^{\mathrm{micro}}_{\mathrm{RL}_n, m} \right] \right] = -\beta^{-1} \ln \mathcal{Z}_n \tag{S56}$$

If all sites are equivalent and interact in the same way with each of the other sites, for instance in a symmetric receptor, then all microscopic configurations of the receptor corresponding to a macroscopic binding state will be equivalent. In this case, the electrochemical potentials of the macroscopic binding state and the microscopic binding states are related by

$$\bar{\mu}_{\mathrm{RL}_n} = \beta \bar{\mu}^{\mathrm{micro}}_{\mathrm{RL}_n} - \ln M\left(n\right) \tag{S57}$$

The total partition function is given by the sum over the Boltzmann factors of all microscopic forms of the receptor. The total number of microscopic states is equal to the sum of the numbers of possible microscopic states for each macroscopic state

$$\mathfrak{N} = \sum_{n=1}^{N} M\left(n\right) \tag{S58}$$

The total partition function is given by

$$\mathcal{Z} = \sum_{n=1}^{\mathfrak{N}} \exp \left[-\beta \bar{\mu}^{\mathrm{micro}}_{n} \right] \tag{S59}$$

The formalism developed for GMCT in the main article allows one to consider a more detailed receptor model in with energetically non-equivalent microstates and different global conformations of the receptor.

C Thermodynamics of transmembrane transport at the example of a monovalent receptor

The chemical potential, $\mu_i = \mu_i^\circ + \beta^{-1} \ln a_i$ of charged species in presence of an electrostatic transmembrane potential aquires an additional term to account for the interaction of its charge distribution with the electrostatic membrane potential. The resulting electrochemical potential is

$$\bar{\mu}_i = \mu_i + z_i \mathrm{e}_\circ \mathrm{N_A} \Theta \Delta\psi \tag{S60}$$

where μ_i is the chemical potential of species i, z_i is the formal charge of the species, $\mathrm{e}_\circ$ is the elementary charge, $\mathrm{N_A}$ is the Avogadro constant, and $\Delta\psi$ is the electrostatic transmembrane potential. According

compound	$\mu^{\circ,(aq)}$ [kcal/mol]	reference
H^+	0	by definition
OH^-	−37.5932	16
H_2O	−56.6874	16
H_3O^+	−54.3682	*
NH_3	−6.35	16
NH_4^+	−18.97	16

Table S4: Standard chemical potentials in water for compounds investigated as potential permeants of the ammonia transporter Amt-1. * calculated from the value for H_2O and the $pKa_1 = 1.7$ (from reference 17) according to Eqs. (S8) and (S13)

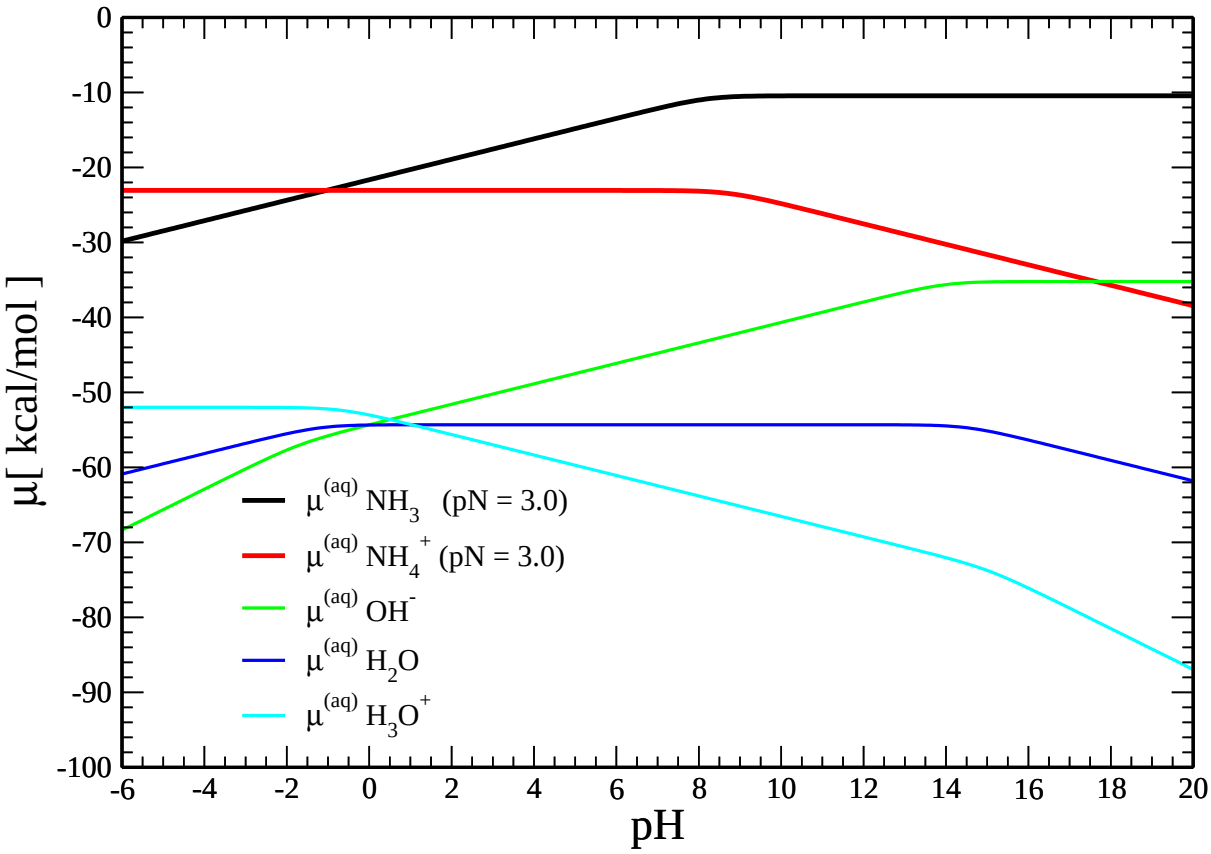

Figure S1: Chemical potential of all permeant species considered in this work as a function of the pH value.

to the electrophysiological convention, $\Delta\psi$ is is measured relative to the outside phase, i.e., it is equal to zero in the bulk outer phase and aquires its full value

$$\Delta\psi = \psi^{\mathrm{in}} - \psi^{\mathrm{out}} \tag{S61}$$

in the bulk inner phase, where bulk means far from the membrane[18]. Consequently, the Heaviside step function Θ adopts a value of 0 in the bulk outside phase and a value of 1 in the bulk inside phase[19]. The free energy change upon transport of the species from the outside to the inside phase is given by the difference in the electrochemical potential of the species between the two phases, i.e., the electrochemical transmembrane gradient of the species

$$\Delta G^{\mathrm{trans}} = \bar{\mu}_i^{\mathrm{in}} - \bar{\mu}_i^{\mathrm{out}} \tag{S62}$$

The transfer free energies for the two species of a monovalent receptor are obtained from Eq. (S62) using Eqs. (S60) and (S4). Substituting the chemical potentials of the receptor species by Eqs. (S26) and (S29), we obtain

$$\Delta G_{\mathrm{R}}^{\mathrm{trans}} = z_{\mathrm{R}}\mathrm{e}_\circ\Delta\psi + \beta^{-1}\ln\left[\frac{a_{\mathrm{RX}}^{\mathrm{in}}}{a_{\mathrm{RX}}^{\mathrm{out}}}\right] + \beta^{-1}\ln\left[\frac{1+\exp\left[-\beta\left(G_i^{\mathrm{int}} - \bar{\mu}_{\mathrm{L}}^{\mathrm{in}}\right)\right]}{1+\exp\left[-\beta\left(G_i^{\mathrm{int}} - \bar{\mu}_{\mathrm{L}}^{\mathrm{out}}\right)\right]}\right] \tag{S63}$$

$$\begin{aligned}\Delta G_{\mathrm{RL}}^{\mathrm{trans}} &= z_{\mathrm{RL}}\mathrm{e}_\circ\Delta\psi + \beta^{-1}\ln\left[\frac{a_{\mathrm{RX}}^{in}}{a_{\mathrm{RX}}^{out}}\right] \\ &+ \beta^{-1}\ln\left[\frac{\left(1+\exp\left[-\beta\left(G_i^{\mathrm{int}} - \bar{\mu}_{\mathrm{L}}^{\mathrm{in}}\right)\right]\right)\exp\left[-\beta\left(G_i^{\mathrm{int}} - \bar{\mu}_{\mathrm{L}}^{\mathrm{in}}\right)\right]}{\left(1+\exp\left[-\beta\left(G_i^{\mathrm{int}} - \bar{\mu}_{\mathrm{L}}^{\mathrm{out}}\right)\right]\right)\exp\left[-\beta\left(G_i^{\mathrm{int}} - \bar{\mu}_{\mathrm{L}}^{\mathrm{out}}\right)\right]}\right]\end{aligned} \tag{S64}$$

Generally, using Eq. (S55) we have for the transfer free energy of the species RL_n of a N valent receptor across the membrane from the outside to the inside phase

$$\Delta G_{\mathrm{RL}_n}^{\mathrm{trans}} = \bar{\mu}_{\mathrm{RL}_n}^{\mathrm{in}} - \bar{\mu}_{\mathrm{RL}_n}^{\mathrm{out}} \tag{S65}$$

where the electrochemical potentials in the two phases are obtained from Eqs. (S60), (S53), (S54) and (S55) using a known membrane potential $\Delta\psi$, known chemical potentials of the ligand and known total concentrations of the receptor in the two phases.

The electrochemical transmembrane gradient of the proton is traditionally termed proton-motive force (pmf). The pmf provides the thermodynamic driving force for many transmembrane transport and other biological processes. The pmf consists of a electrical component and a chemical component. The chemical component is often expressed in terms of a transmembrane pH difference. Equivalently to the convention adopted for the electric transmembrane potential, the transmembrane pH-difference is defined as[18]

$$\Delta\mathrm{pH} = \mathrm{pH}^{\mathrm{in}} - \mathrm{pH}^{\mathrm{out}} \tag{S66}$$

The pmf in terms of ΔpH and $\Delta\psi$ is given by

$$\begin{aligned}\mathrm{pmf} = &\quad -\frac{\ln 10}{\beta\mathrm{F}}\Delta\mathrm{pH} + \Delta\psi \\ \approx &\quad -59\,\mathrm{mV}\;\Delta\mathrm{pH} + \Delta\psi\end{aligned} \tag{S67}$$

D Electrostatic potential plots

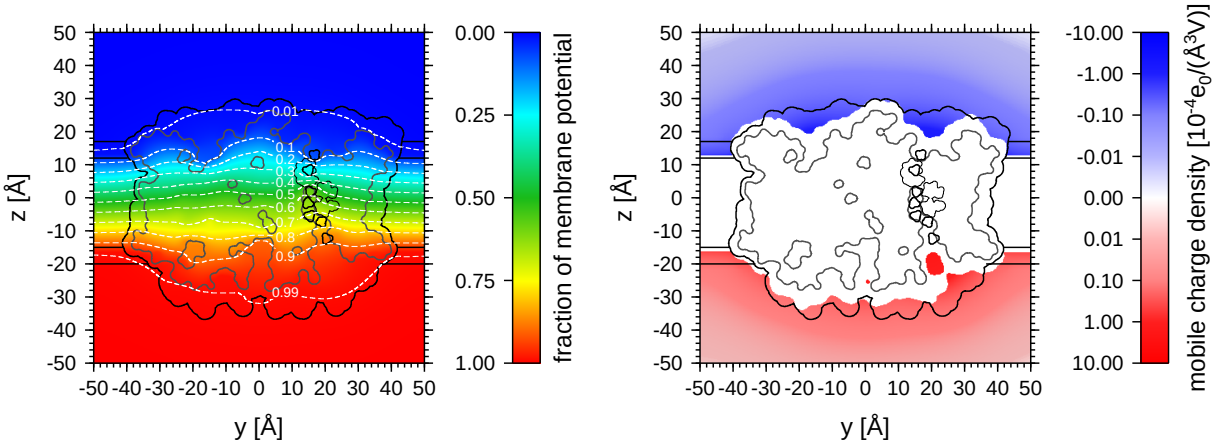

Figure S2: Fraction of the electrostatic transmembrane potential in a cross-section through AfAmt-1 as function of the transverse position z and the lateral position y in the projection plane. The orientation of the protein and the slice plane are the same as in Fig. 4 of the main text.

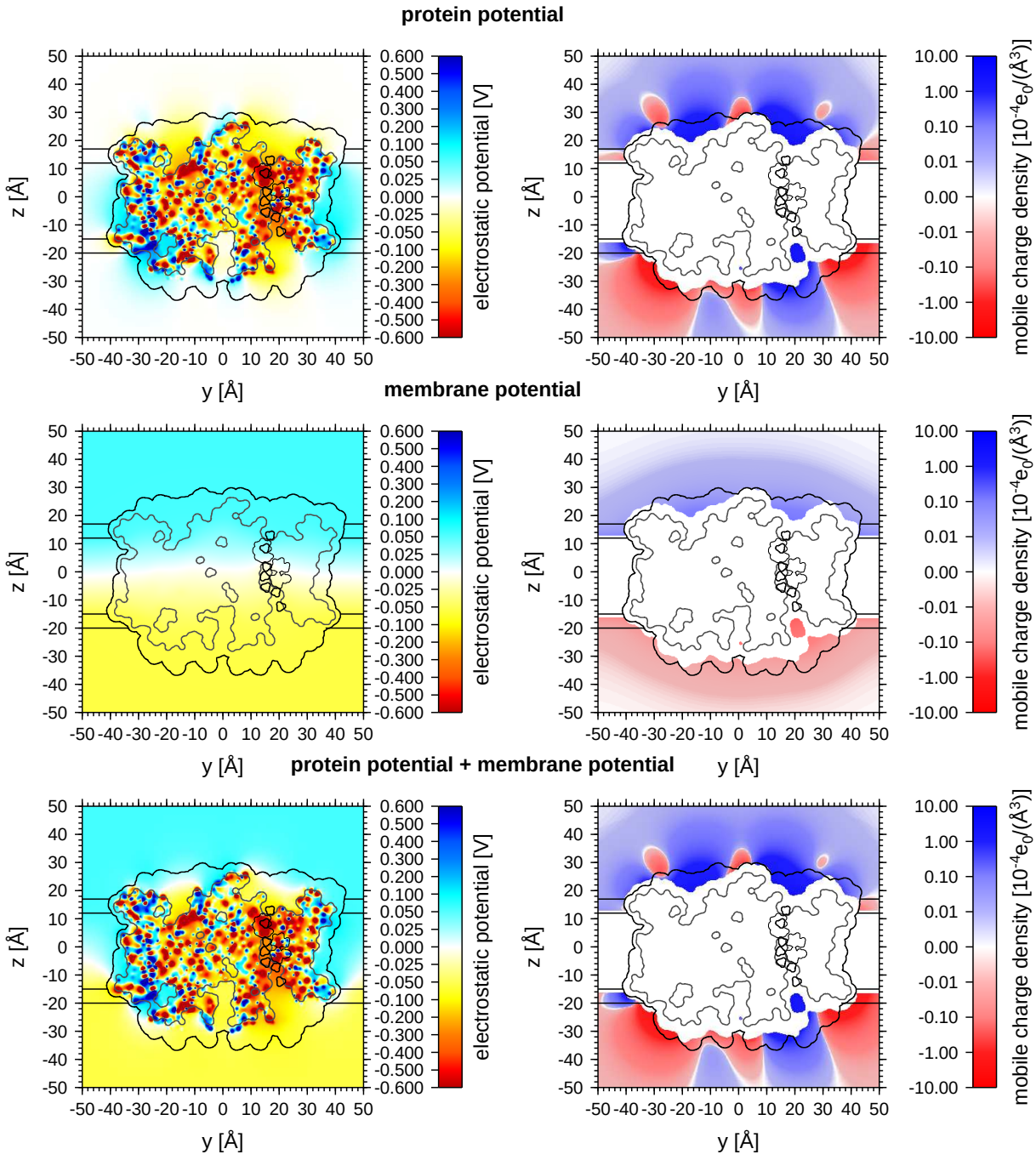

Figure S3: Electrostatic potential distribution, overall view. The electrostatic potential and the corresponding mobile charge density in a cross-section through AfAmt-1 plotted as functions of the transverse position z and the lateral position y in the projection plane. The orientation of the protein and the slice plane are the same as in Fig. 4 of the main text. The electrostatic potentials are plotted in the same slice plane. **b)** The electrostatic potential under typical conditions (pH = 7.0 and $\Delta\psi = -0.12$ V). The structure of AfAmt-1 was constructed by setting all sites to their most highly populated instances under the specified conditions. The electrostatic potential and the mobile charge density are color coded (see color bars). left column: electrostatic potential right column: mobile charge density top row: electrostatic potential originating from the protein charge distribution and the corresponding mobile charge density induced by the electrostatic potential of Amt-1 in the solvent. middle row: electrostatic transmembrane potential and the corresponding mobile source charge distribution bottom row: sum of top and middle rows

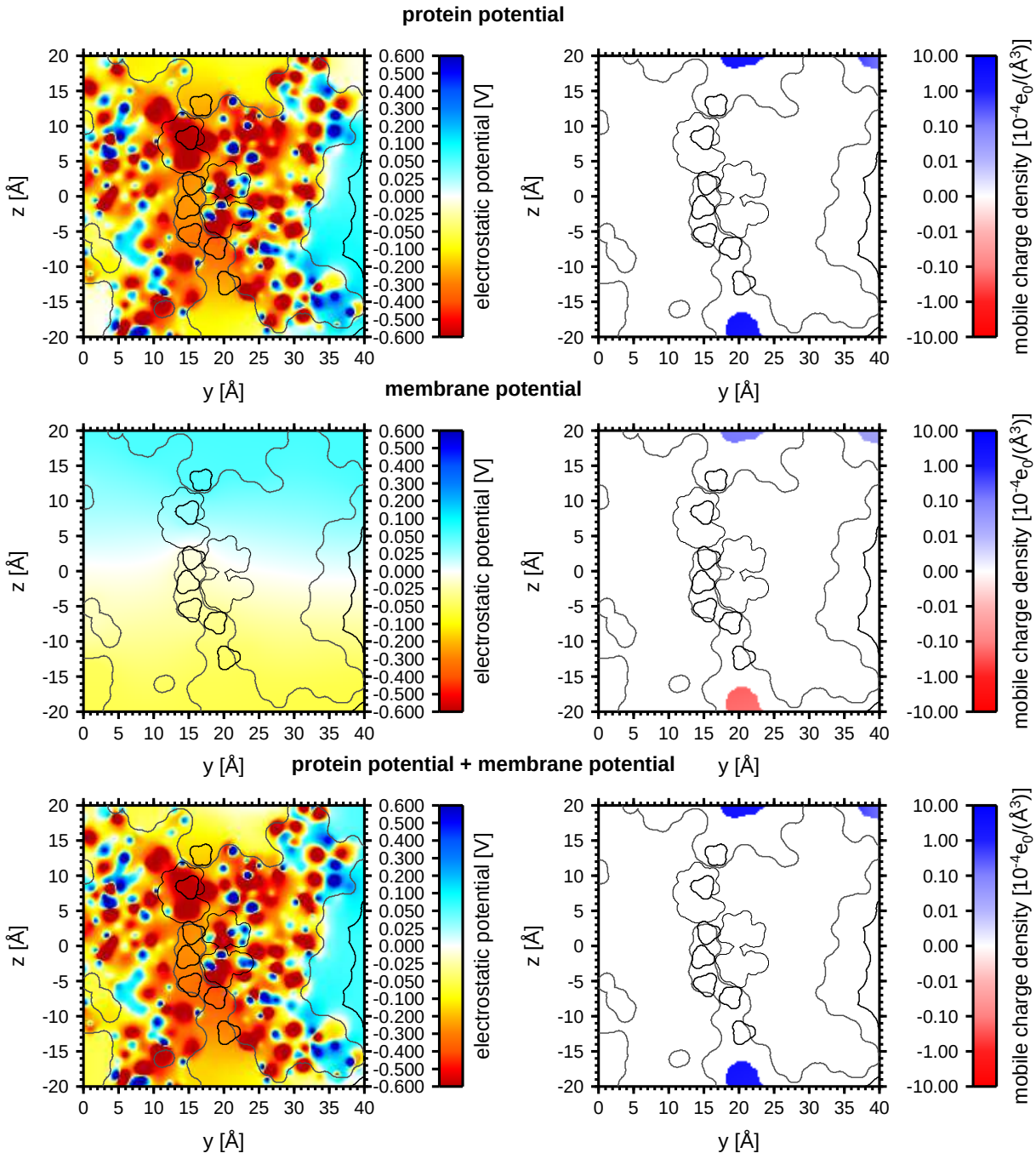

Figure S4: Electrostatic potential distribution, magnified view of the transmembrane pore region. Otherwise the plots are equivalent to those of Fig. S3. See caption of Fig. 4 for explanation.

E Titration curves

Figures. S5 to S8 show titration curves as function of intracellular pH value and the transmembrane pH difference. The transmembrane pH difference is defined by Eq. (S66). The transmembrane pH difference is expressed in terms of a proton-motive force (pmf) using Eq. (S67). This representation of the pH gradient facilitates the comparison of the effects of electrical and chemical components of the electrochemical transmembrane gradient of the proton. A pmf consisting purely of a pH difference can be converted to ΔpH by a conversion factor of $\approx -1/59$ mV.

Most notable is the highly irregular titration behavior of H157 and H305 which form the twin-His motif. Almost over the entire titration region, there is a significant probability for the deprotonated and the protonated form of these sites This titration behavior shows that the protonated and deprotonated forms are separated by a small free energy difference over wide ranges of pH and transmembrane pH difference.

There are multiple residues with carboxylic acid side chains on the extracellular surface of Amt-1 whose protonation probability is increased by moderate negative transmembrane pH differences. Thus, the negative charge on the extracellular side decreases if the extracellular pH value decreases. The decrease in the extracellular pH value does also increase the driving force for the import of protons and ammonium ions and the abundance of protons in the extracellular phase. The protonation of the extracellular carboxylic acid sidechains would lead to a decreased attraction of the positively charged ammonium ions or protons by AfAmt-1. Thus, the protonation of the carboxylic acid sidec chains on the extracellular surface could be a mechanism to regulate the influx of the ammonium ion or even protons if the pH gradient becomes too high. This regulation could prevent an excessive rise of the intracellular ammonium concentrations that could be toxic for the cell. In addition, the regulation mechanism could prevent an excessive influx of protons through the ammonium transporter and subsequent overacidification of the intracellular phase if the extracellular phase is very acidic.

Figures. S9 to S12 show titration curves as function of the intracellular pH value and the electric transmembrane potential. The transmembrane potential is defined by Eq. (S61). H157 and H305 exhibit a similarly highly irregular titration behavior as in case of the pH-ΔpH titration, which shows that the protonated and deprotonated forms are separated by a small free energy difference over almost the entire titration region considered. A highly similar titration behavior is also observed in case of a compound pmf with a typical ratio of the pmf contributions of the pH gradient and the transmembrane potential as depicted in Figures. S13 to S16.

Figures. S17 to S24 show titration curves as function of pH value and the pN value in absence or presence of a typical pmf. It can be seen that the binding probabilities of ammonium or ammonia at the permeant sites are small for realistic pN values (pN > 0). This binding behavior is caused by the much larger abundance of water which competes for the permeant sites. Because of the high water activity, all permeant sites are almost fully occupied by water. A tight binding of ammonium or ammonia to the permeant sites would require entirely unrealistic values of pN $<$ pO, i.e., the replacement of the aquaeous solvent phases by a concentrated solution of ammonium/ammonia.

The most interesting titration behavior of protonatable amino acid residues is again exhibited by H157 and H305. The twin-His residues are the only residues which show a strong dependence of their protonation behavior on the occupation of the permeant sites by ammonium or ammonia. In addition, these residues retain significant probabilities of beeing protonated and of beeing deprotonated over most of the titration region considered. Thus, the protonation states of the twin-His residues are also separated by a low free energy difference if the permeant sites are occupied by ammonium or ammonia. Thus, H157 and H305 can easily change their protonation state over the entire region of physiologically relevant conditions. Because of this ability, it seems atrractive to consider a possible active role of the twin-His motif in the conduction mechanism of AfAmt-1.

For all titrations, there are two lysine residues at the interface of the membrane headgroup and core regions that are predicted to be deprotonated already at unusually low pH values (K292 and K361). For K292, this behavior is mainly caused by the close proximity of the sidechain of K293. The sidechains of K292 and K293 can thus be considered to share a proton. The amino group of K361 is located within the core region immediately at the interface to the headgroup region. The protonation behavior of K361 may thus be an artifact of the simulation setup caused by the uncertainty in the thickness

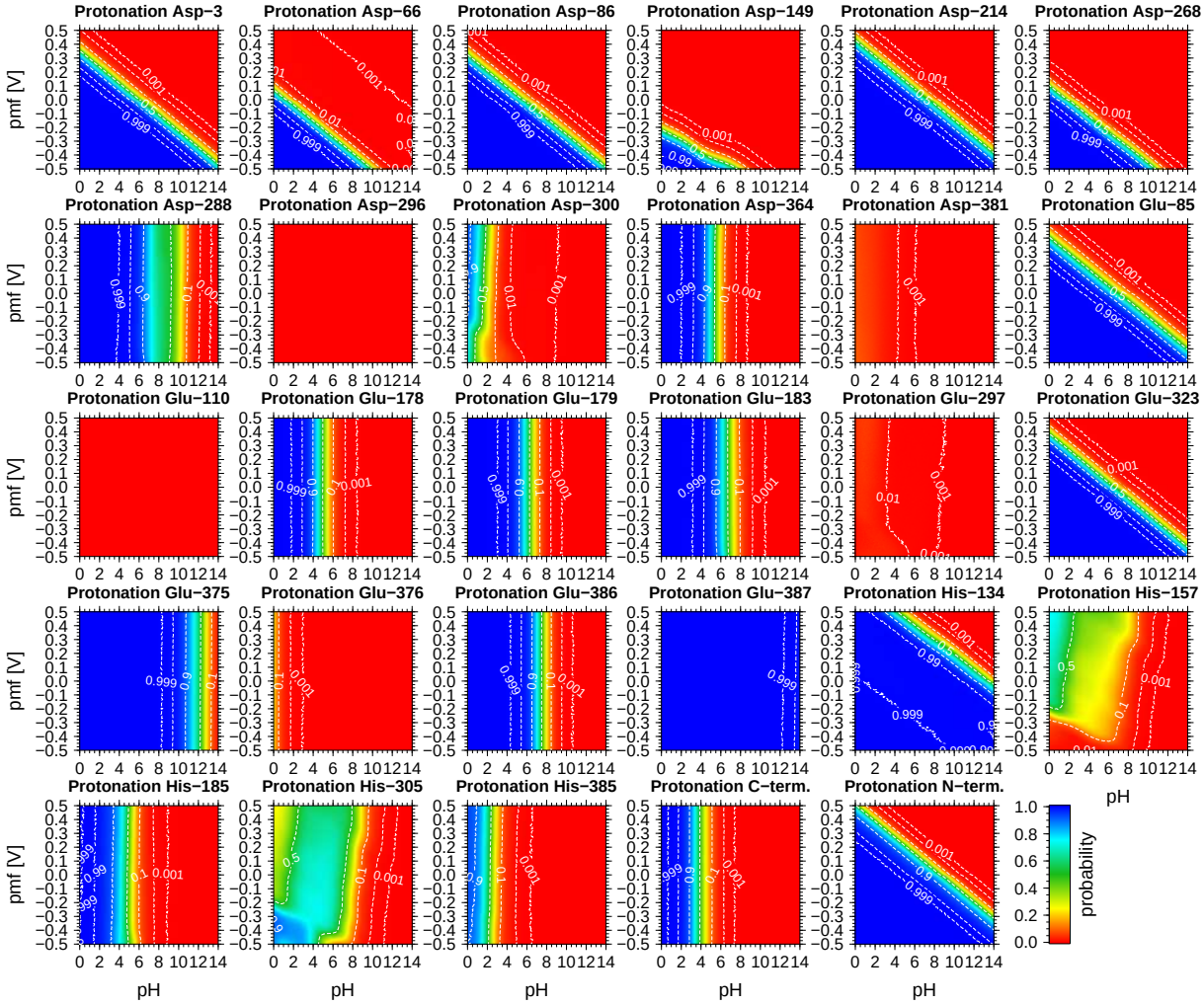

Figure S5: Titration curves pH - ΔpH I. Protonation probability as a function of the intracellular pH value and a pmf consisting entirely of a transmembrane pH difference. The sites are indicated by the labels above the curves. The protonation probability is color coded (see color bar) and indicated by isocontours. Protonation of histidine residues refers to binding of a proton to one of the singly protonated charge-neutral tautomers to form the doubly protonated positively charged imidazolium form.

and position of the membrane core regions. The sidechain conformation adopted by K361 in the lipid depleted crystal environment may also differ from the conformation adopted in the native membrane environment. However, the location of K361 is far from the transmembrane pore of AfAmt-1. Thus, a possible artifactually favored deprotonation of K361 does not affect the behavior of the mechanistically important sites in the vincinity of the transmembrane pore.

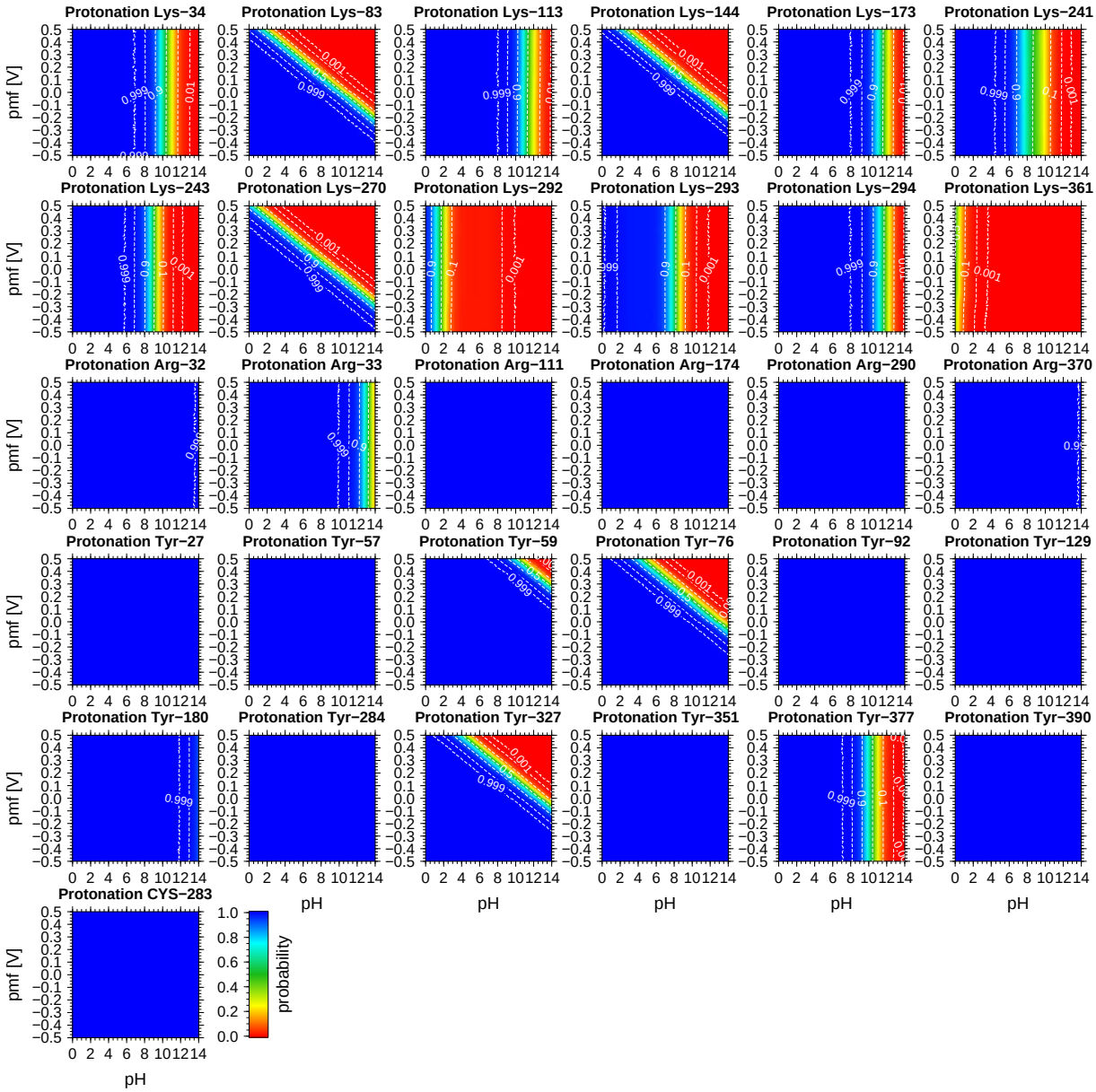

Figure S6: Titration curves pH - ΔpH II.. Continued from Fig. S5. See caption of Fig. S5 for explanation.

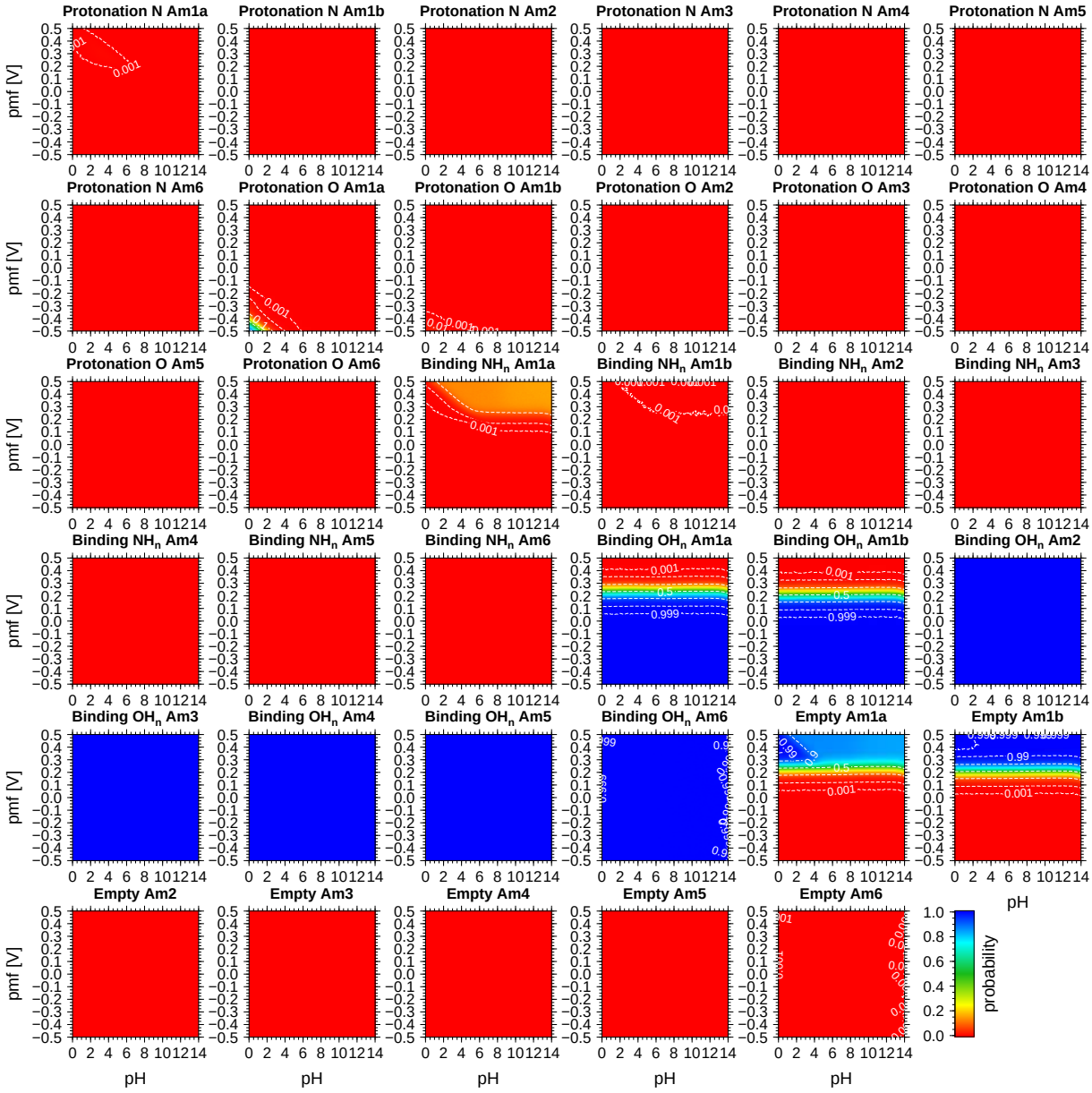

Figure S7: Titration curves pH - ΔpH III. Probability for binding states of the sites in the transmembrane pore. as a function of the intracellular pH value and a pmf consisting entirely of a transmembrane pH difference. The sites and the specific binding probabilities are indicated by the labels above the curves. Protonation N indicates the conditional probability of binding an ammonium ion under the condition that either ammonium or ammonium is bound to the site. Protonation N indicates the conditional probability of binding an hydronium ion under the condition that either water or an hydronium ion is bound to the site. Binding NH_n indicates the probability of binding ammonia or an ammonium ion to the site. Binding OH_n indicates the probability of binding any water species (water, hydronium ion or hydroxide ion) to the site.

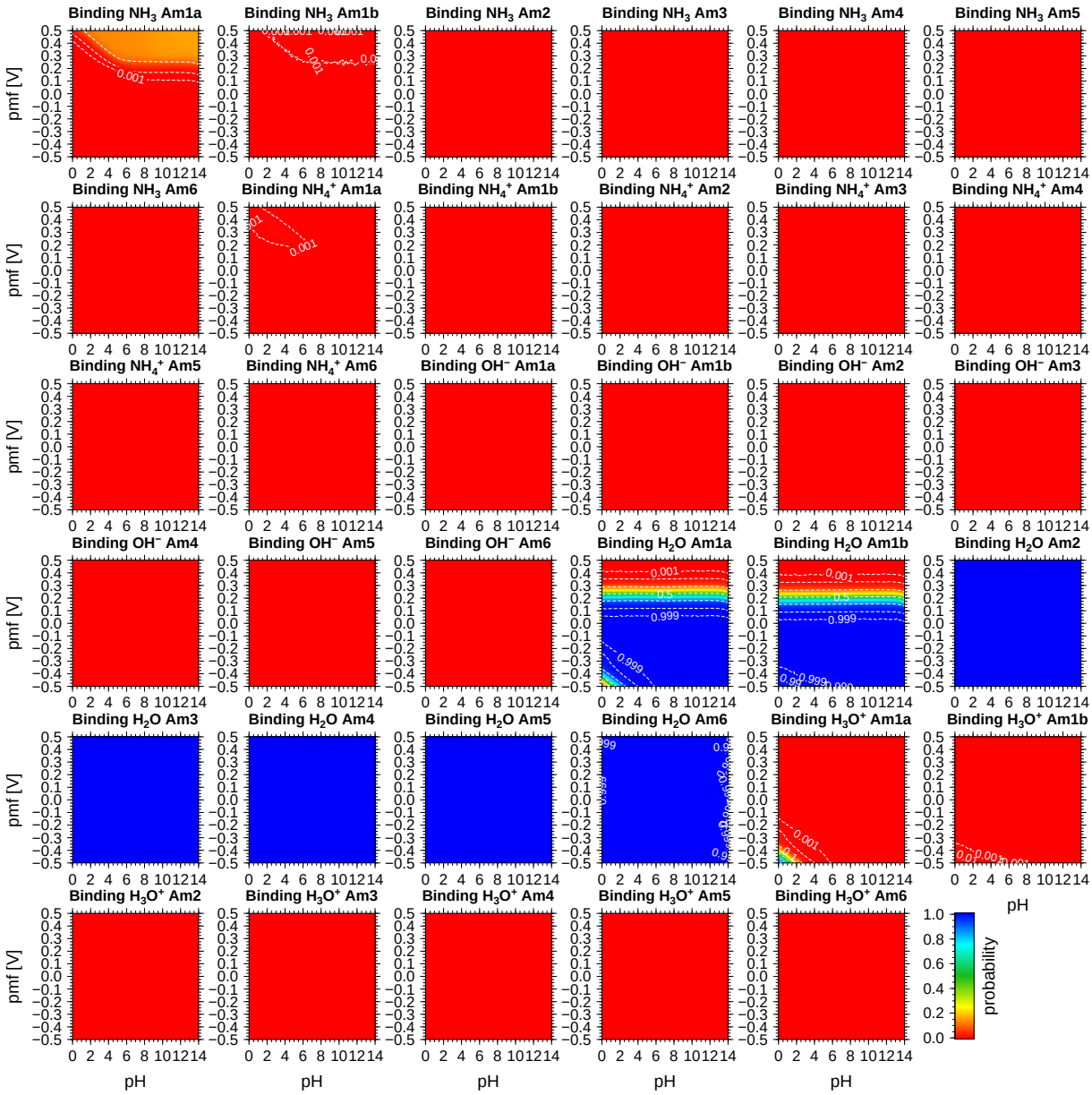

Figure S8: Titration curves pH - ΔpH IV. Continued from Fig. S7. See caption of Fig. S7 for explanation.

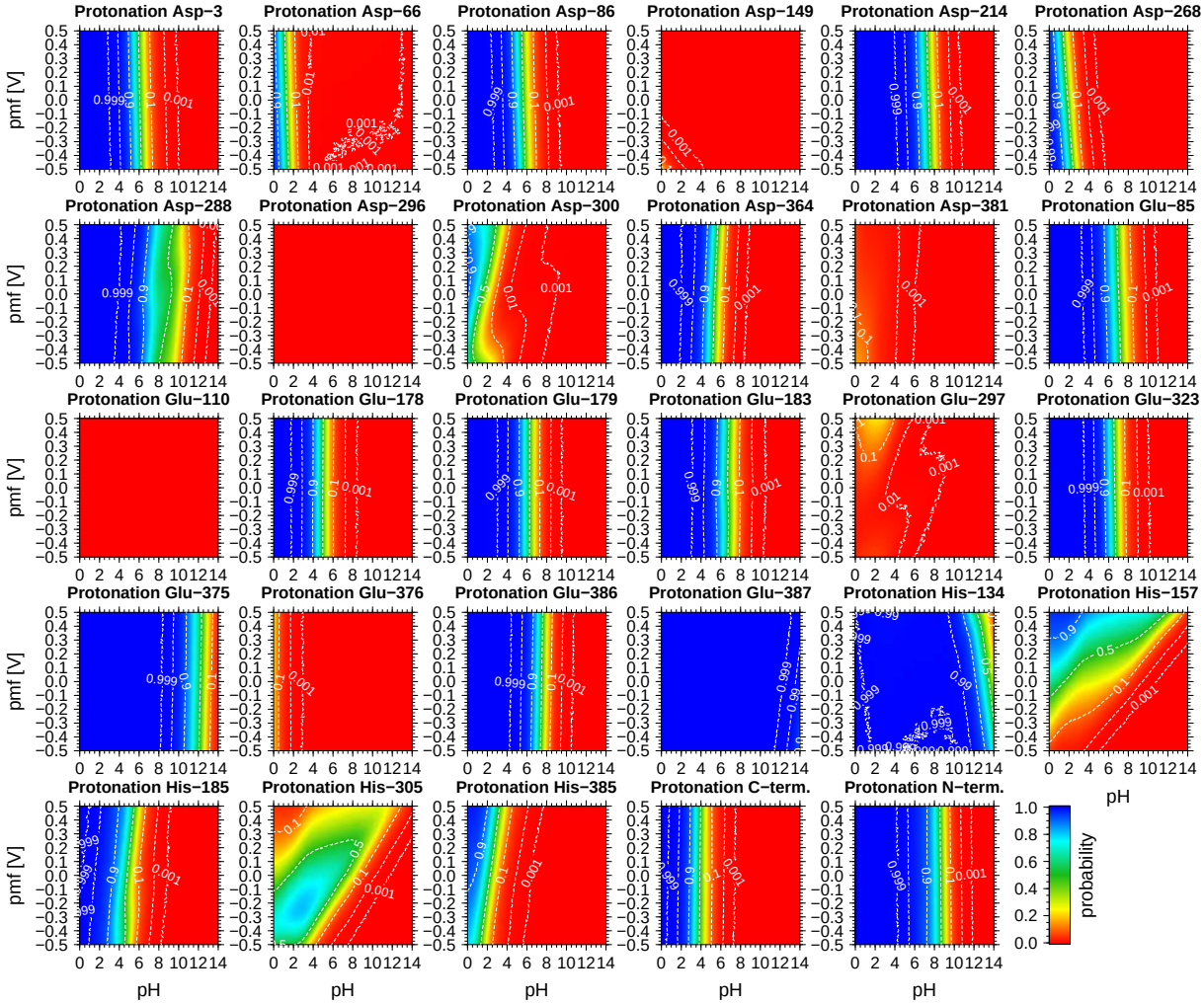

Figure S9: Titration curves pH - $\Delta\psi$ I. Protonation probability as a function of the intracellular pH value and a pmf consisting entirely of an electric transmembrane potential. The sites are indicated by the labels above the curves. The protonation probability is color coded (see color bar) and indicated by isocontours. Protonation of histidine residues refers to binding of a proton to one of the singly protonated charge-neutral tautomers to form the doubly protonated positively charged imidazolium form.

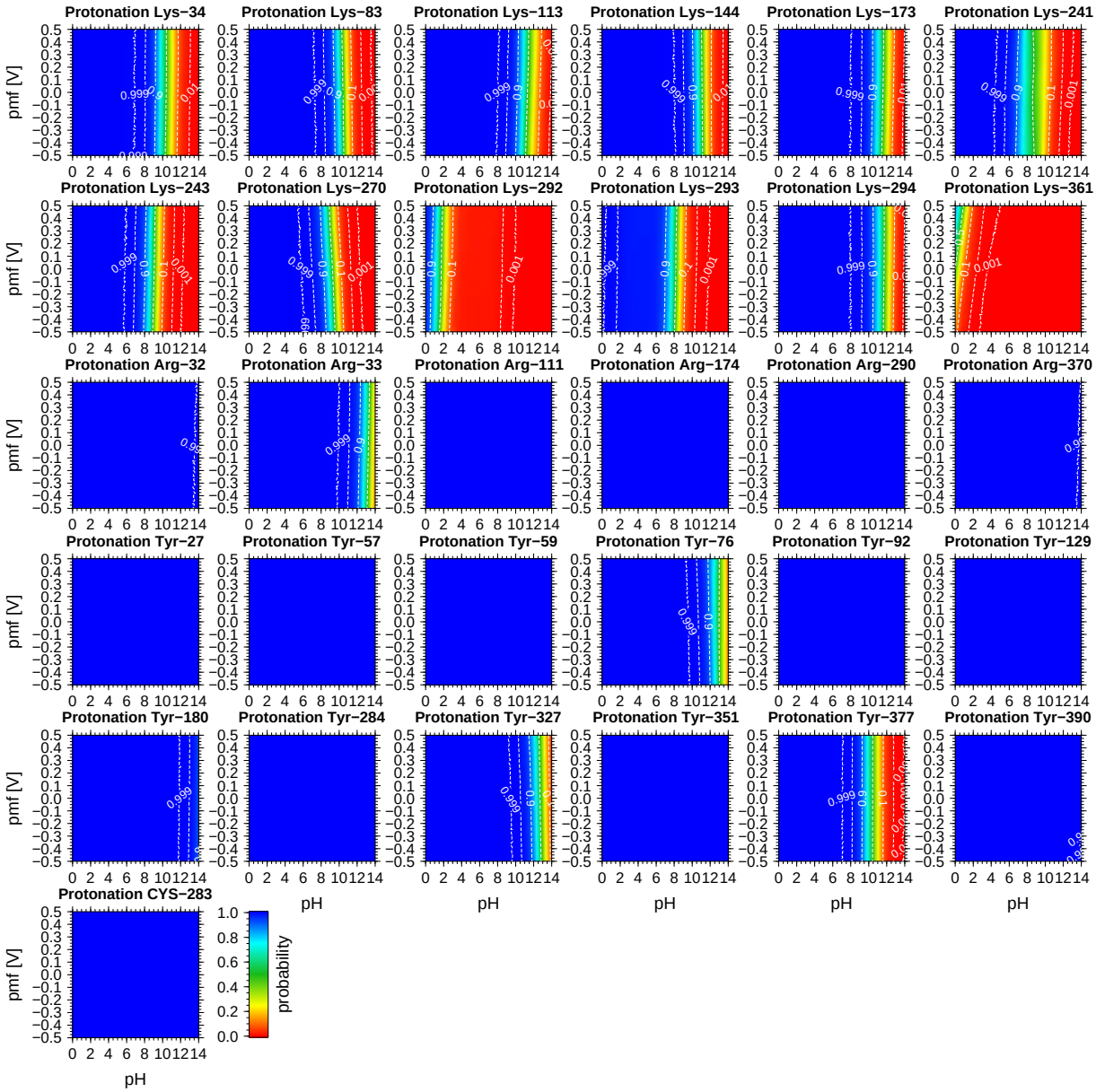

Figure S10: Titration curves pH - $\Delta\psi$ II. Continued from Fig. S9. See caption of Fig. S9 for explanation.

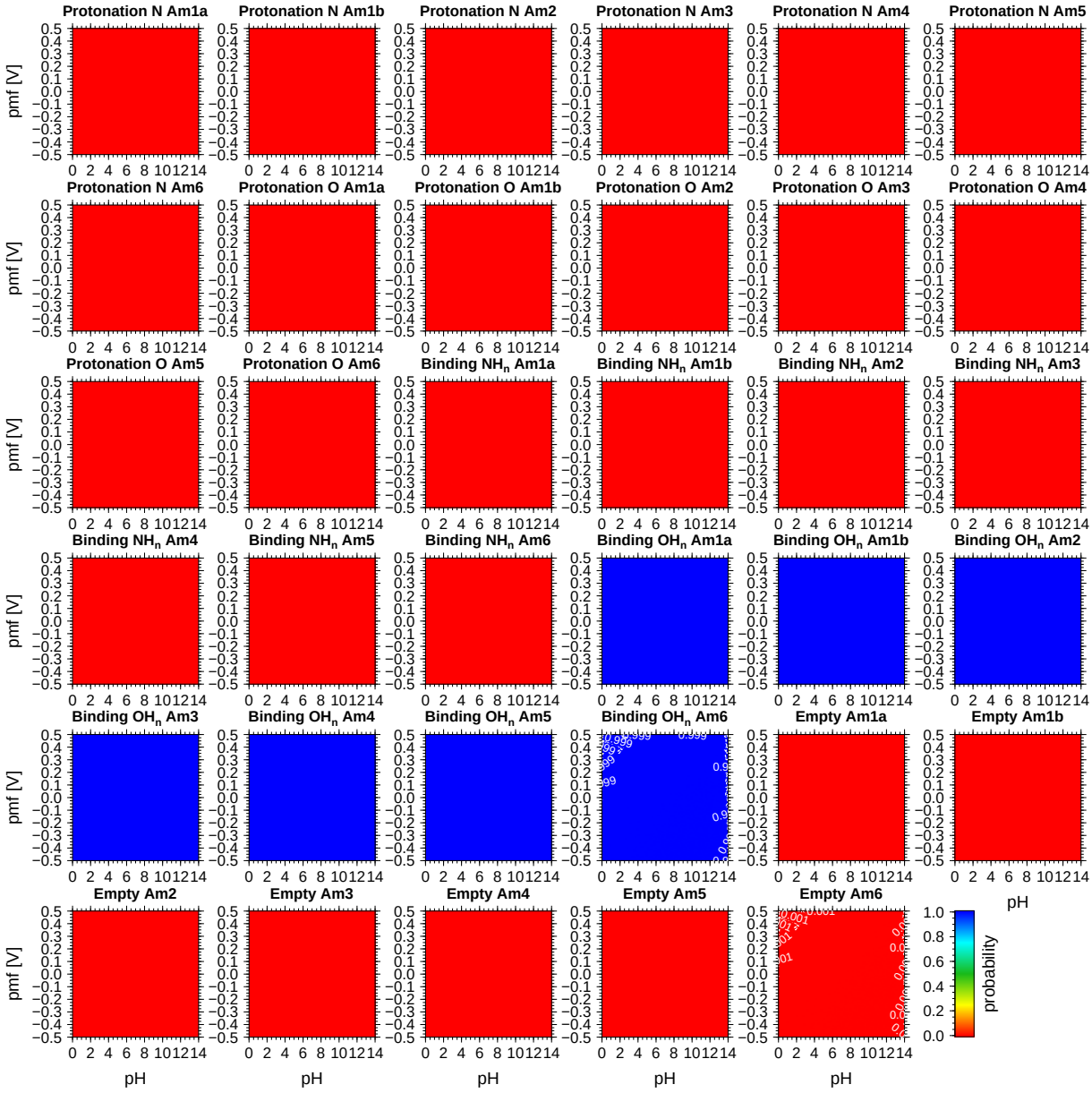

Figure S11: Titration curves pH - $\Delta\psi$ III. Probability for binding states of the sites in the transmembrane pore as a function of the intracellular pH value and a pmf consisting entirely of an electric transmembrane potential. The sites and the specific binding probabilities are indicated by the labels above the curves. Protonation N indicates the conditional probability of binding an ammonium ion under the condition that either ammonium or ammonium is bound to the site. Protonation N indicates the conditional probability of binding an hydronium ion under the condition that either water or an hydronium ion is bound to the site. Binding NH_n indicates the probability of binding ammonia or an ammonium ion to the site. Binding OH_n indicates the probability of binding any water species (water, hydronium ion or hydroxide ion) to the site.

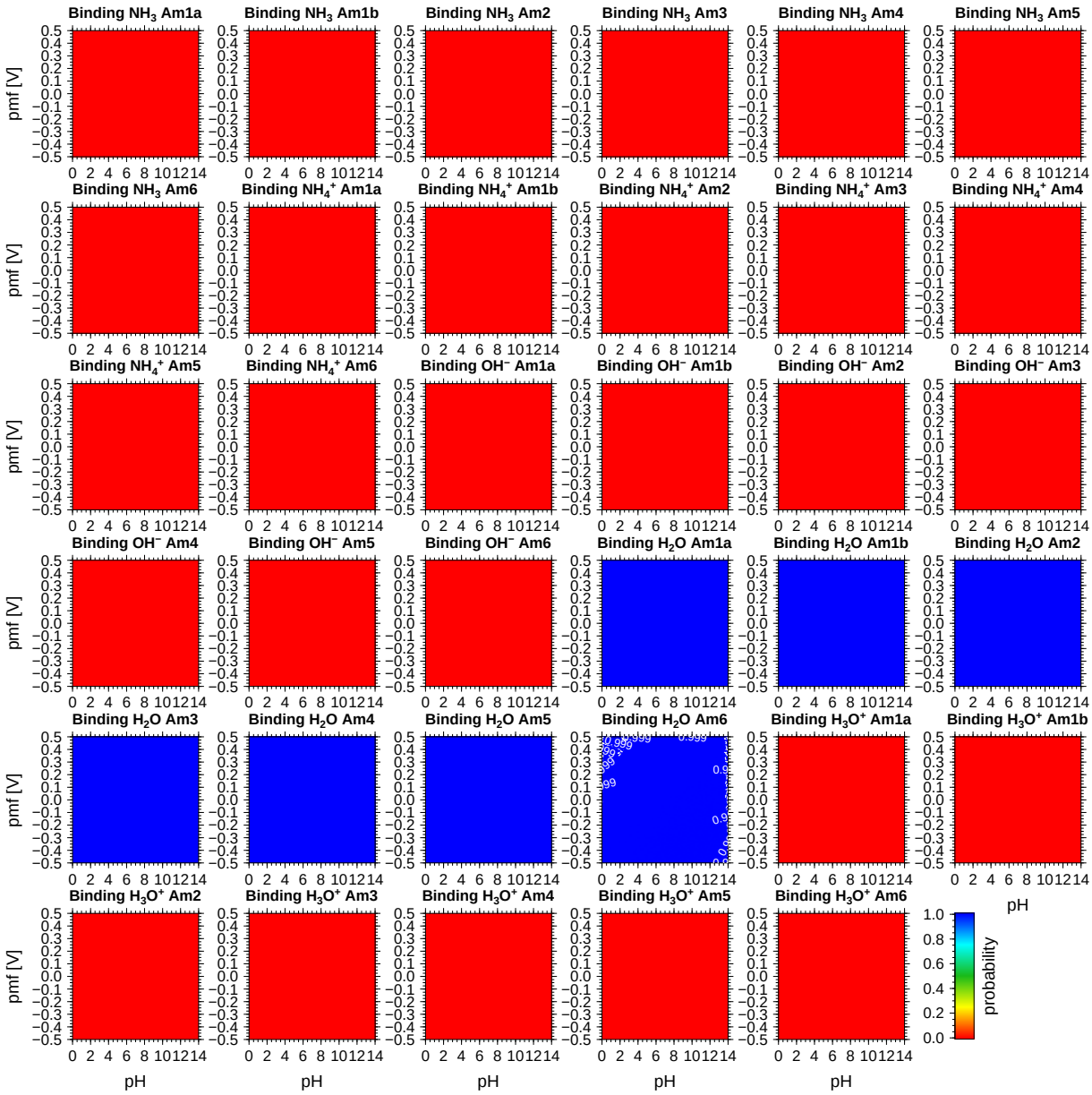

Figure S12: Titration curves pH - $\Delta\psi$ IV. Continued from Fig. S11. See caption of Fig. S11 for explanation.

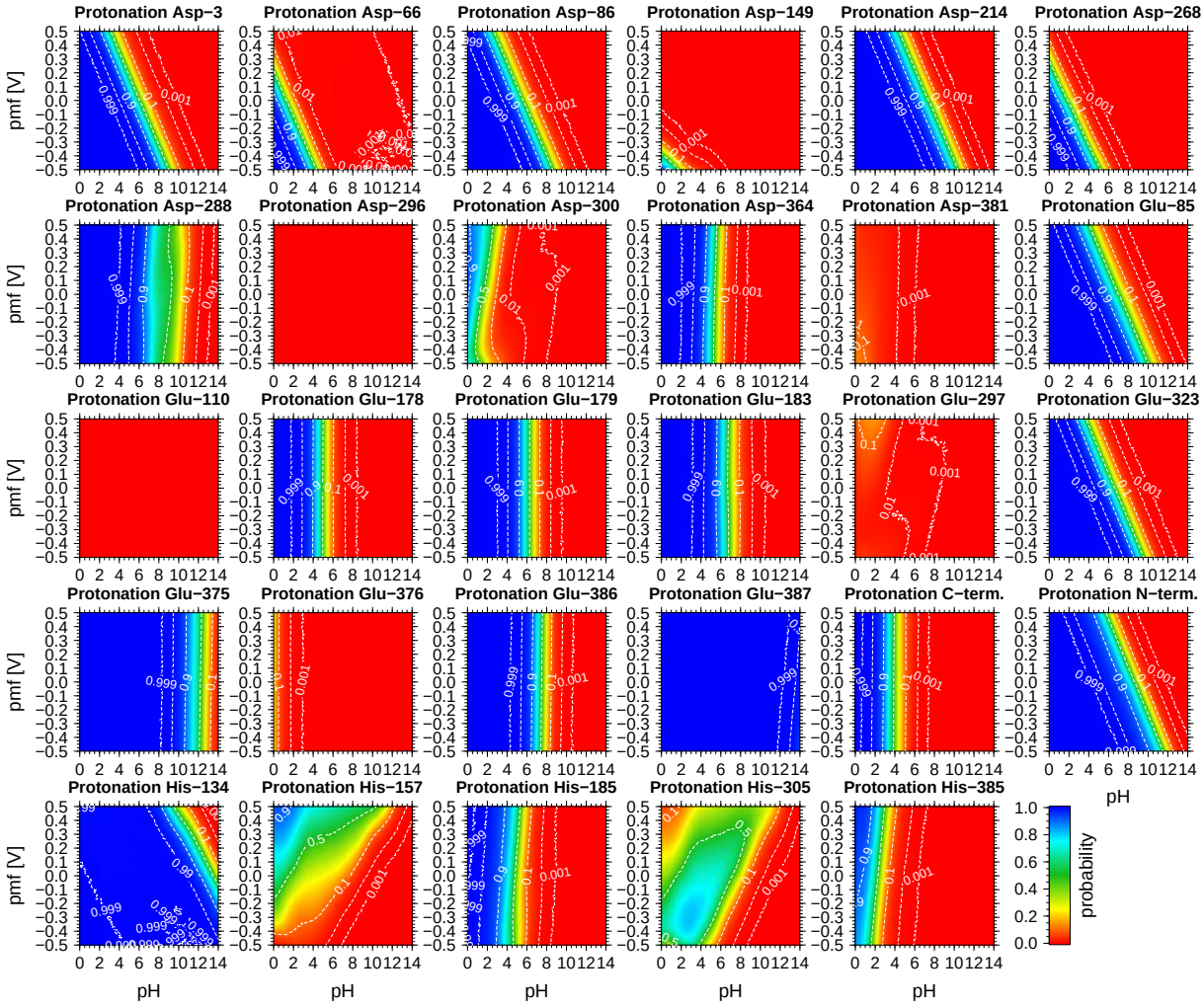

Figure S13: Titration curves pH - ΔpH $+\Delta\psi$ I. Protonation probability as a function of the intracellular pH value and a pmf consisting of a transmembrane pH difference and an electric transmembrane potential. The ratio of the pH difference to the electric transmembrane potential is given by $\frac{\Delta\psi}{\Delta\mathrm{pH}} = 2$. The sites are indicated by the labels above the curves. The protonation probability is color coded (see color bar) and indicated by isocontours. Protonation of histidine residues refers to binding of a proton to one of the singly protonated charge-neutral tautomers to form the doubly protonated positively charged imidazolium form.

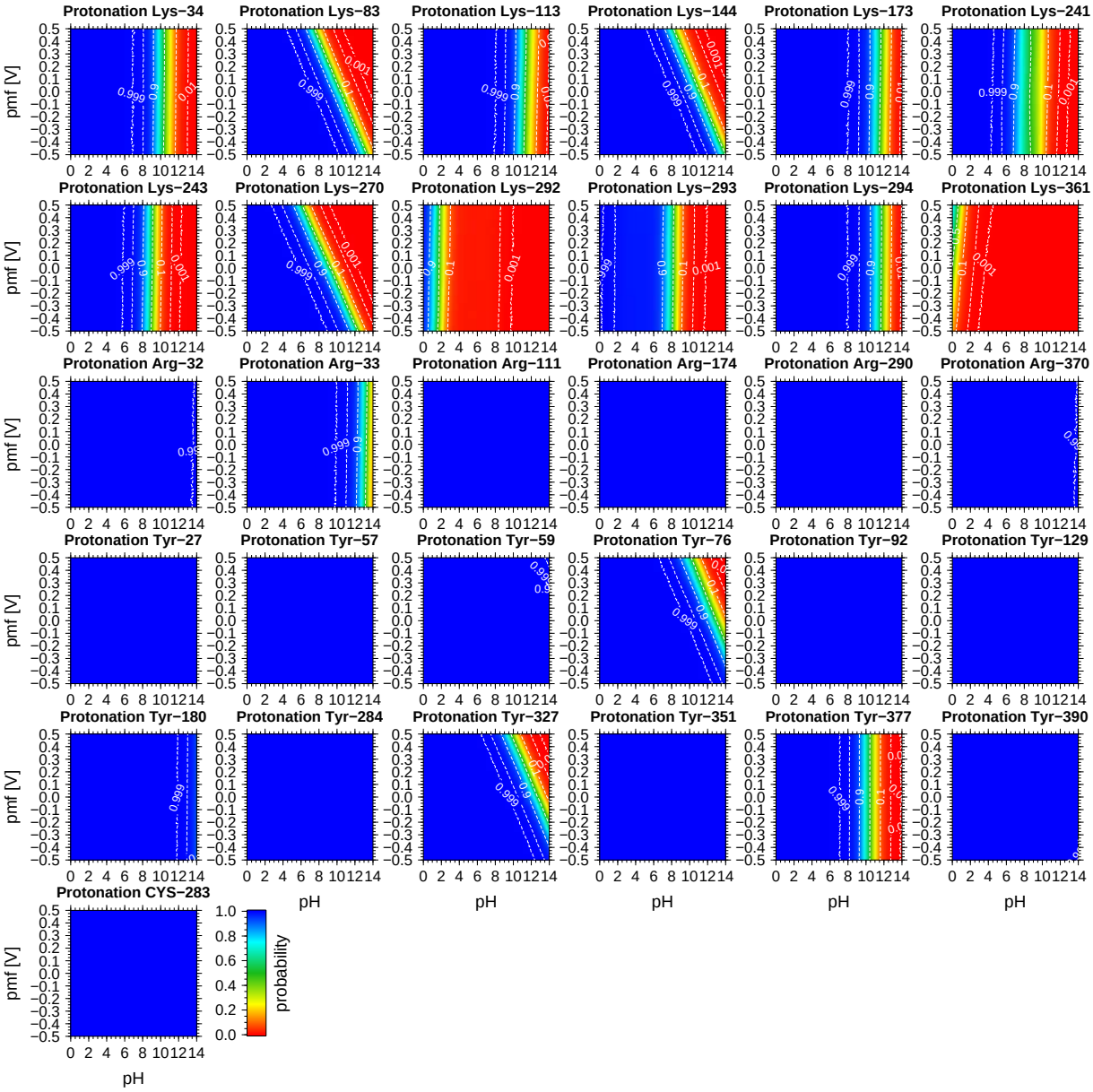

Figure S14: Titration curves pH - ΔpH +Δψ II. Continued from Fig. S13. See caption of Fig. S13 for explanation.

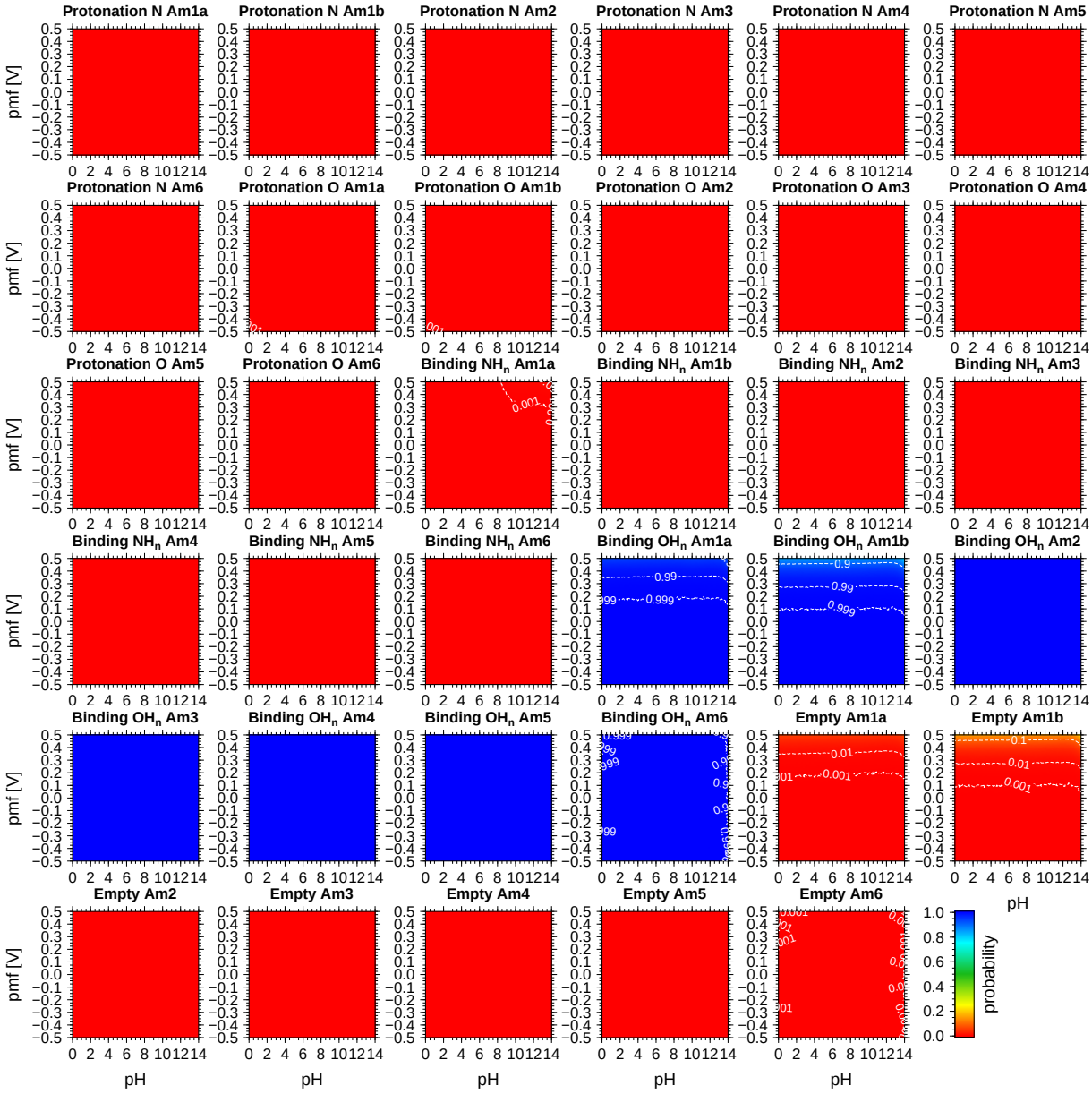

Figure S15: Titration curves pH - ΔpH +Δψ III. Probability for binding states of the sites in the transmembrane pore as a function of the intracellular pH value and a pmf consisting of a transmembrane pH difference and an electric transmembrane potential. The ratio of the pH difference to the electric transmembrane potential is given by $\frac{\Delta\psi}{\Delta\mathrm{pH}} = 2$. The sites and the specific binding probabilities are indicated by the labels above the curves. Protonation N indicates the conditional probability of binding an ammonium ion under the condition that either ammonium or ammonium is bound to the site. Protonation N indicates the conditional probability of binding an hydronium ion under the condition that either water or an hydronium ion is bound to the site. Binding NH_n indicates the probability of binding ammonia or an ammonium ion to the site. Binding OH_n indicates the probability of binding any water species (water, hydronium ion or hydroxide ion) to the site.

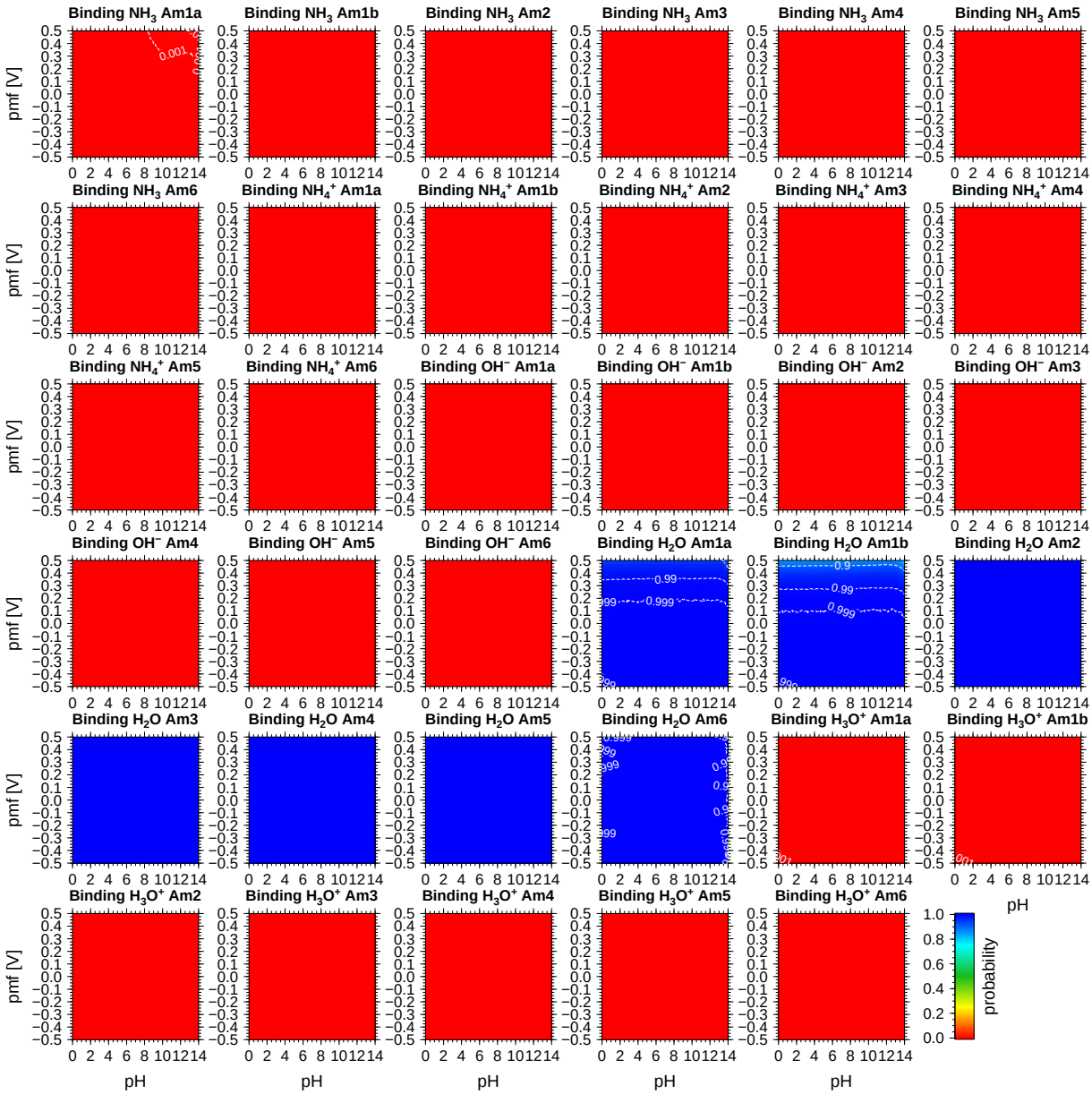

Figure S16: Titration curves pH - ΔpH $+\Delta\psi$ IV. Continued from Fig. S15. See caption of Fig. S15 for explanation.

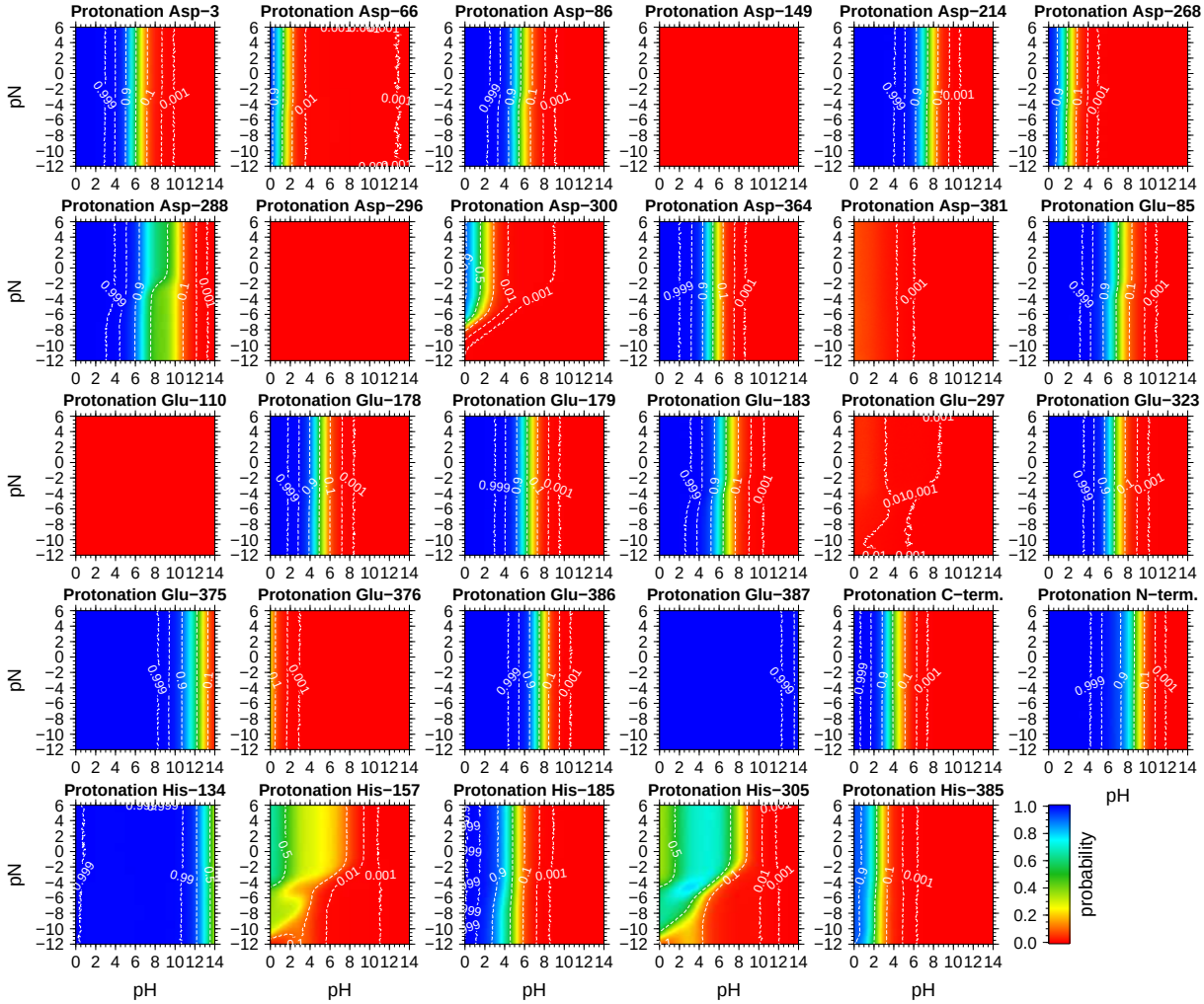

Figure S17: Titration curves intracellular pH - pN without pmf I. (pN equal on both membrane sides). Protonation probability as a function of the intracellular pH value and a pmf consisting of a transmembrane pH difference and an electric transmembrane potential. The ratio of the pH difference to the electric transmembrane potential is given by $\frac{\Delta\psi}{\Delta\mathrm{pH}} = 2$. The sites are indicated by the labels above the curves. The protonation probability is color coded (see color bar) and indicated by isocontours. Protonation of histidine residues refers to binding of a proton to one of the singly protonated charge-neutral tautomers to form the doubly protonated positively charged imidazolium form.

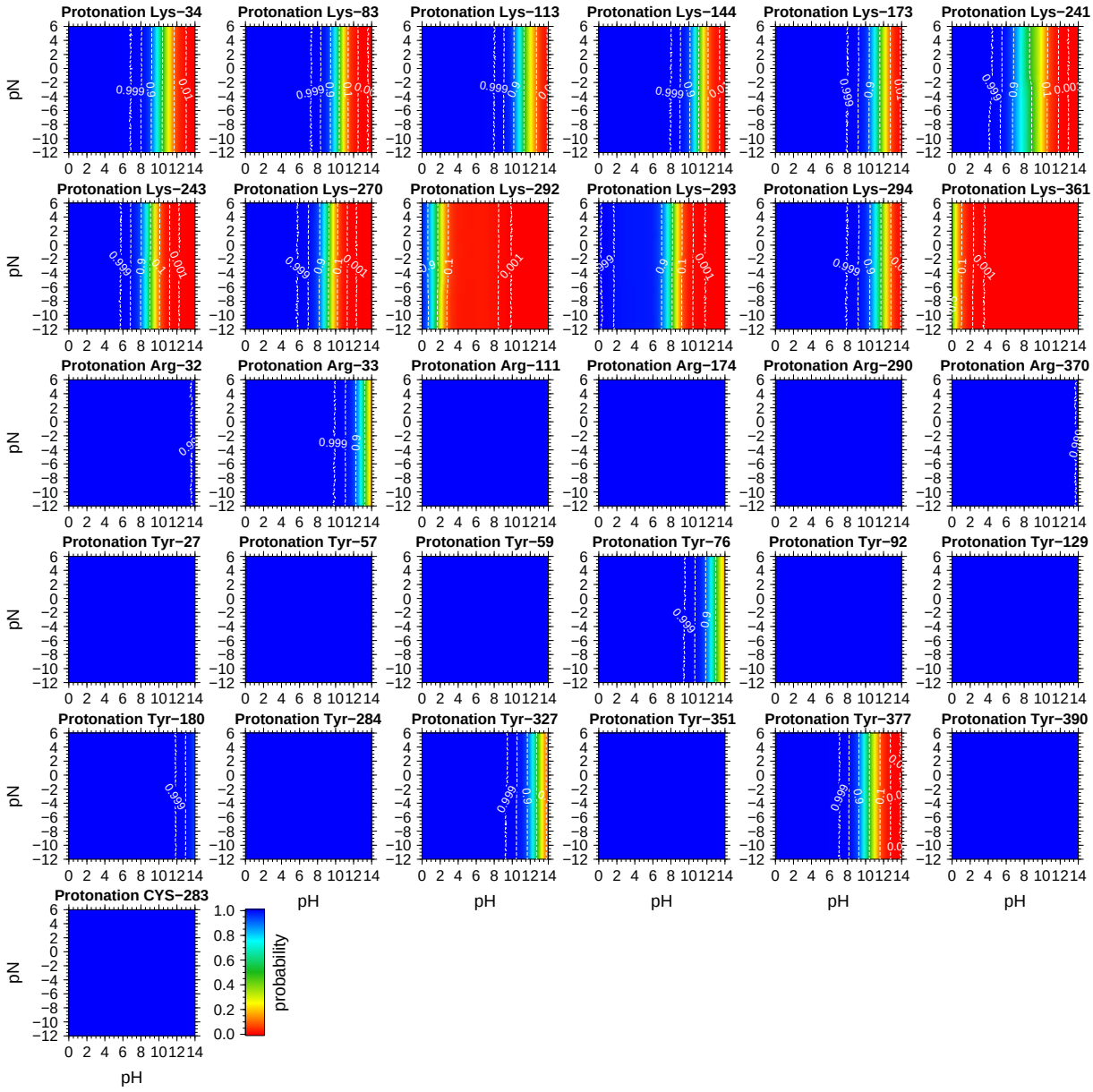

Figure S18: Titration curves pH - pN without pmf II. Continued from Fig. S17. See caption of Fig. S17 for explanation.

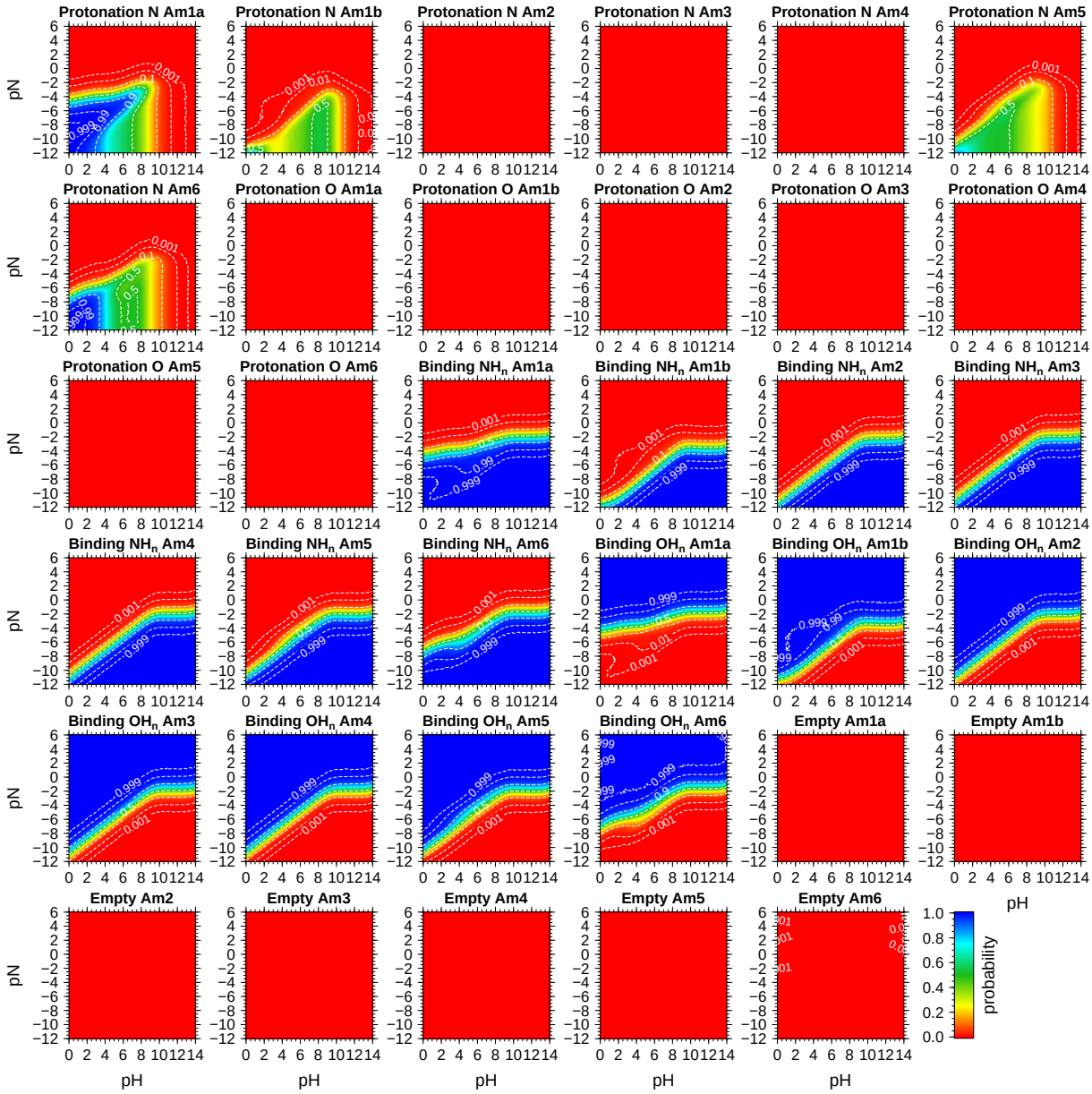

Figure S19: Titration curves pH - pN without pmf III. (pN equal on both membrane sides). Probability for binding states of the sites in the transmembrane pore as a function of the intracellular pH value and a pmf consisting of a transmembrane pH difference and an electric transmembrane potential. The ratio of the pH difference to the electric transmembrane potential is given by $\frac{\Delta\psi}{\Delta\mathrm{pH}} = 2$. The sites and the specific binding probabilities are indicated by the labels above the curves. Protonation N indicates the conditional probability of binding an ammonium ion under the condition that either ammonium or ammonium is bound to the site. Protonation N indicates the conditional probability of binding an hydronium ion under the condition that either water or an hydronium ion is bound to the site. Binding NH_n indicates the probability of binding ammonia or an ammonium ion to the site. Binding OH_n indicates the probability of binding any water species (water, hydronium ion or hydroxide ion) to the site.

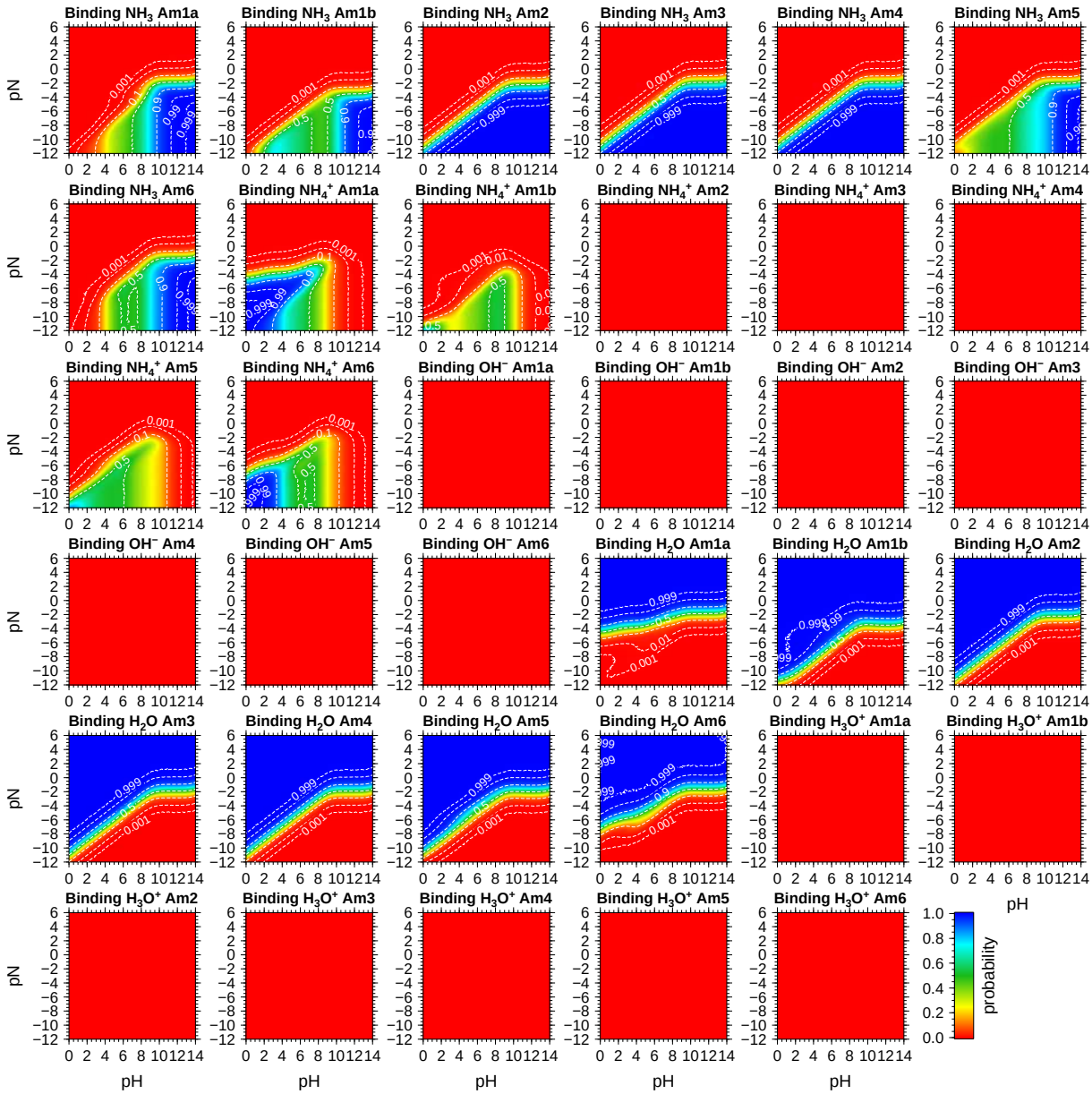

Figure S20: Titration curves pH - pN without pmf IV. Continued from Fig. S19. See caption of Fig. S19 for explanation.

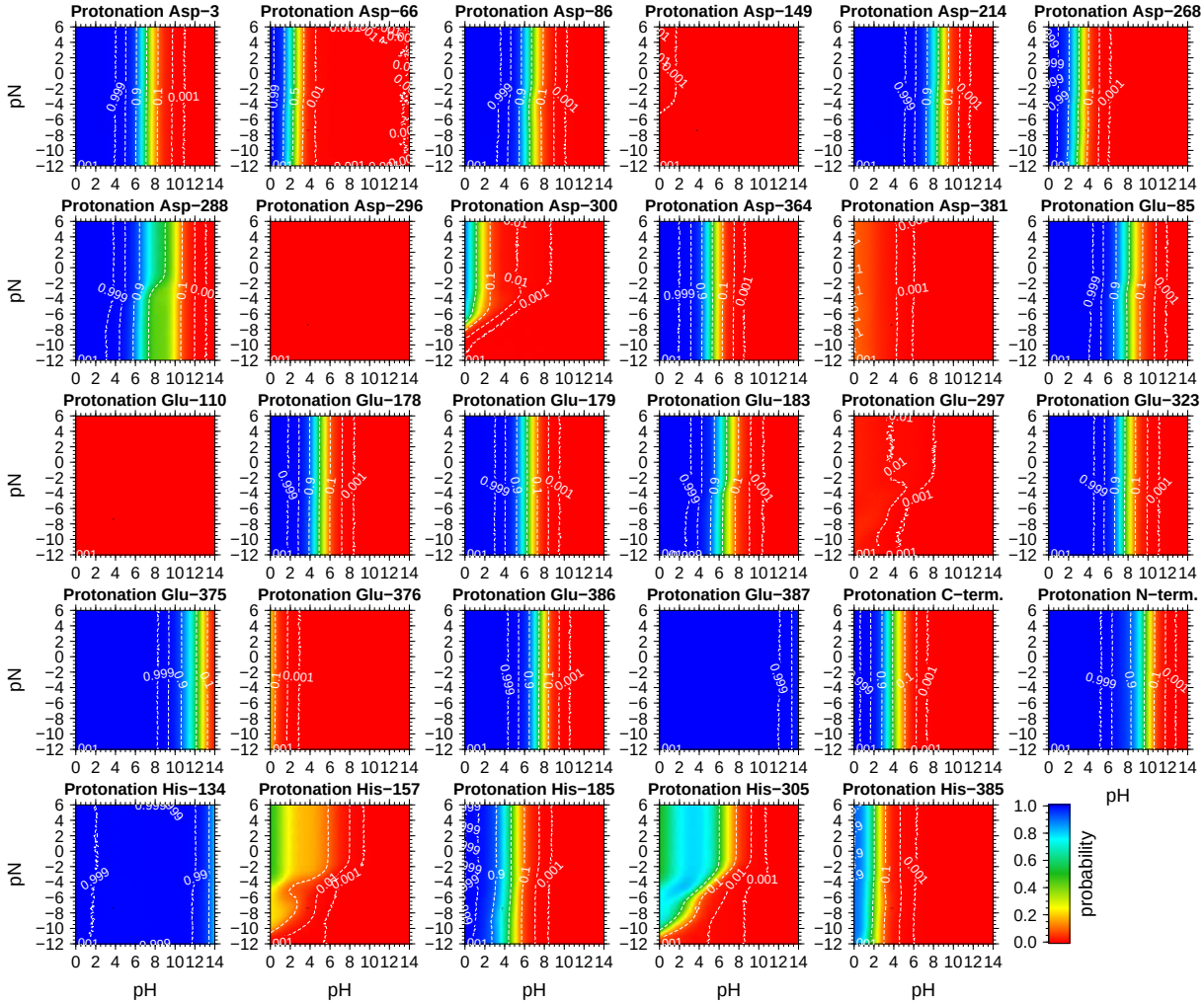

Figure S21: Titration curves intracellular pH - pN with pmf I. (pN equal on both membrane sides, ΔpH= 1.0, $\Delta\psi = -120$ mV). Protonation probability as a function of the intracellular pH value and a pmf consisting of a transmembrane pH difference and an electric transmembrane potential. The ratio of the pH difference to the electric transmembrane potential is given by $\frac{\Delta\psi}{\Delta\mathrm{pH}} = 2$. The sites are indicated by the labels above the curves. The protonation probability is color coded (see color bar) and indicated by isocontours. Protonation of histidine residues refers to binding of a proton to one of the singly protonated charge-neutral tautomers to form the doubly protonated positively charged imidazolium form.

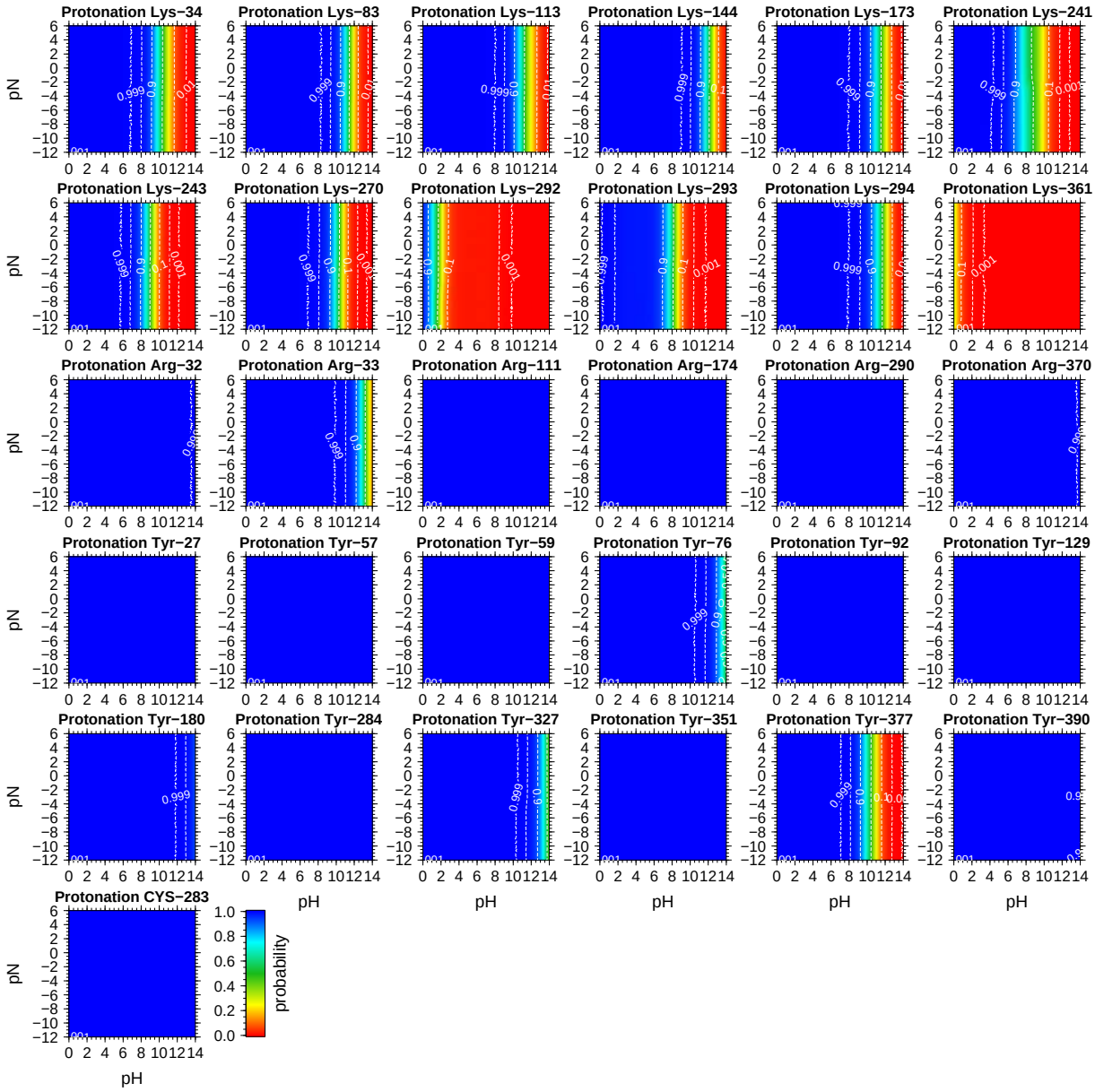

Figure S22: Titration curves intracellular pH - pN with pmf II., (pN equal on both membrane sides, ΔpH= 1.0, $\Delta\psi = -120$ mV). Continued from Fig. S21. See caption of Fig. S21 for explanation.

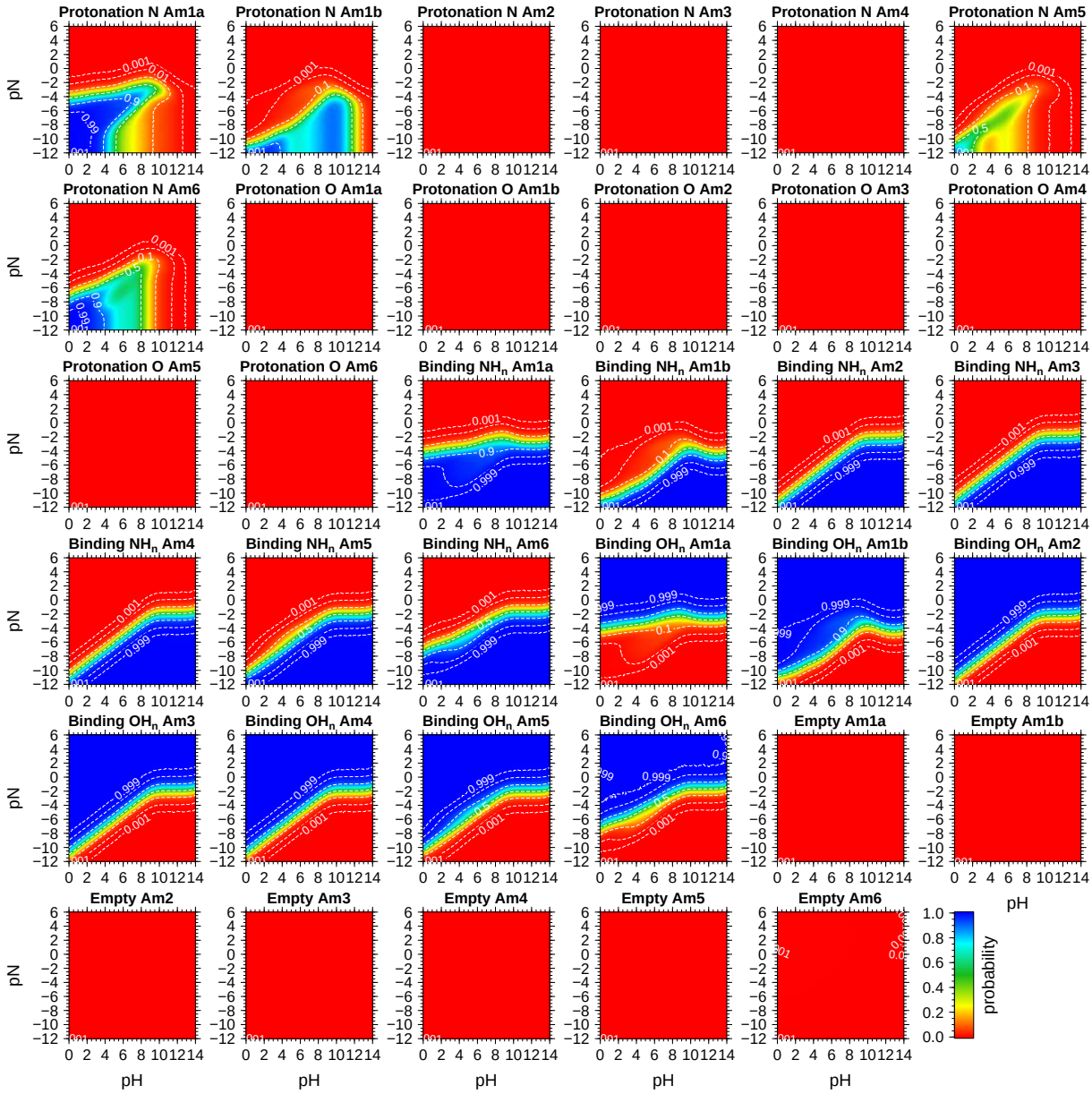

Figure S23: Titration curves intracellular pH - pN with pmf III., (pN equal on both membrane sides, ΔpH= 1.0, $\Delta\psi = -120$ mV). Probability for binding states of the sites in the transmembrane pore as a function of the intracellular pH value and a pmf consisting of a transmembrane pH difference and an electric transmembrane potential. The ratio of the pH difference to the electric transmembrane potential is given by $\frac{\Delta\psi}{\Delta\text{pH}} = 2$. The sites and the specific binding probabilities are indicated by the labels above the curves. Protonation N indicates the conditional probability of binding an ammonium ion under the condition that either ammonium or ammonium is bound to the site. Protonation N indicates the conditional probability of binding an hydronium ion under the condition that either water or an hydronium ion is bound to the site. Binding NH$_n$ indicates the probability of binding ammonia or an ammonium ion to the site. Binding OH$_n$ indicates the probability of binding any water species (water, hydronium ion or hydroxide ion) to the site.

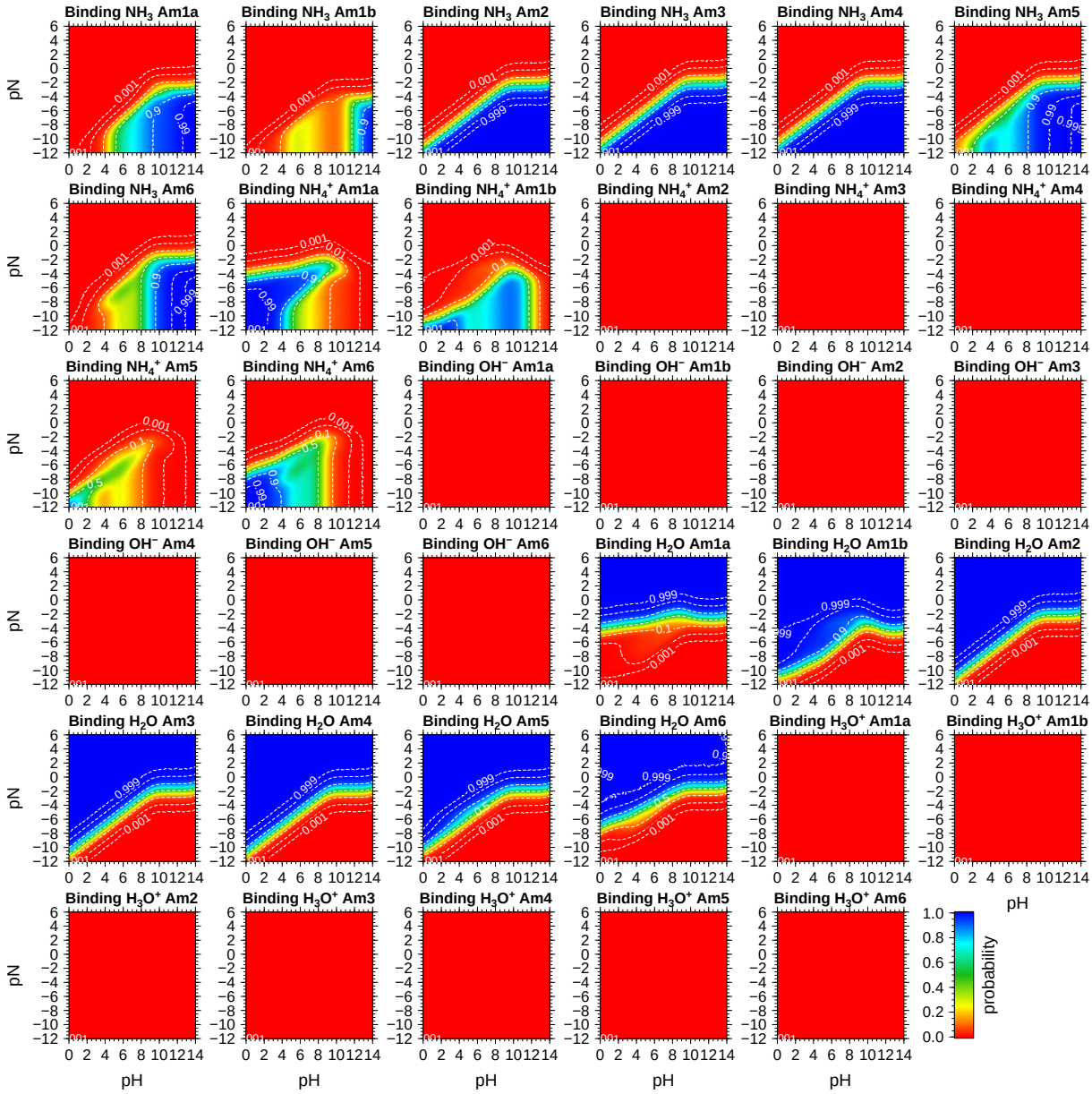

Figure S24: Titration curves intracellular pH - pN with pmf IV., (pN equal on both membrane sides, ΔpH= 1.0, $\Delta\psi = -120$ mV). Continued from Fig. S23. See caption of Fig. S23 for explanation.

F Binding free energy plots

This section contains plots of the binding free energies for all permeant sites as a function of the electrical and chemical components of the pmf. Figure S25 shows plots of the binding free energy for the considered permeant species at all permeant sites as functions of an electric transmembrane potential or a transmembrane pH gradient. The intracellular pH value is fixed to 7.0 and the pN is set to 3.0 on both membrane sides. The binding free energy of the charged permeants is affected by $\Delta\psi$, while that of the uncharged permeants is not directly affected. The small influence of $\Delta\psi$ on the binding free energy of the uncharged permeants are caused by interactions with other binding sites that are sensitive to $\Delta\psi$. The electric transmembrane potential favors the uptake of cations from the membrane side with the positive electrostatic potential and their release to the membrane side with the negative potential. Conversely, $\Delta\psi$ favors the uptake of anions from the membrane side with the positive electrostatic potential and their release to the opposite membrane side. A physiological transmembrane potential ($\Delta\psi < 0$) favors the uptake of positively charged permeants from the outside phase and their release to the inside phase.

The transmembrane pH gradient only affects the two permeant sites in the extracellular vestibule (Am1a and Am1b) directly, because the intracellular pH value is held constant. The binding free energies at the extracellular vestibule are affected directly because a change in the extracellular pH value alters the permeant activities in the extracellular phase as discussed above. If the pH adopts values significantly above the pK_a value of ammonium, ammonia will be the predominant protonation form. Thus, small pH changes in this region will only have a major effect on the activity of ammonium but not on the activity of ammonia. Consequently, the binding free energy of ammonia is insensitive to the pH value in the alkaline pH region, while the corresponding binding free energy of ammonium is roughly linearly dependent on the pH value. If the extracellular pH adopts values significantly below the pK_a of ammonium, ammonium will be the predominant protonation form. Thus, small pH changes in this region will only have a major effect on the activity of ammonia but not on the activity of ammonium. In effect, the binding free energy of ammonium is insensitive to the pH value in the pH region well below 9.25, while the corresponding binding free energy of ammonia is roughly linearly dependent on the extracellular pH value. Similar considerations apply to the dependence of the binding free energies of the protonation forms of water on their activities. Figure S1 of the Supporting Information shows plots of the permeant chemical potentials as functions of the pH value to illustrate the effect of the pH value.

Besides the effect on the permeant electrochemical potentials, the pmf components do also influence the intrinsic energies of the binding sites. A change in the binding form of the protein sites does in turn influence the magnitude of their interaction energy with the permeant sites. The magnitude of these interactions is largest for the charged permeant species due to the dominant contribution of the electrostatic interactions. The complex network of interactions of the binding sites sites causes the non-linear dependence of some of the computed binding free energies on the pmf components. The site-site interactions are also the reason for the weak dependence of some of the binding free energies at the intracellular sites on the pH gradient that determines the extracellular pH value. These interactions are not restricted to a small set of other binding sites but include small contributions from many binding sites. The apolar membrane environment enhances this effect because it leads to a longer range of electrostatic interactions than a purely aqueous environment.

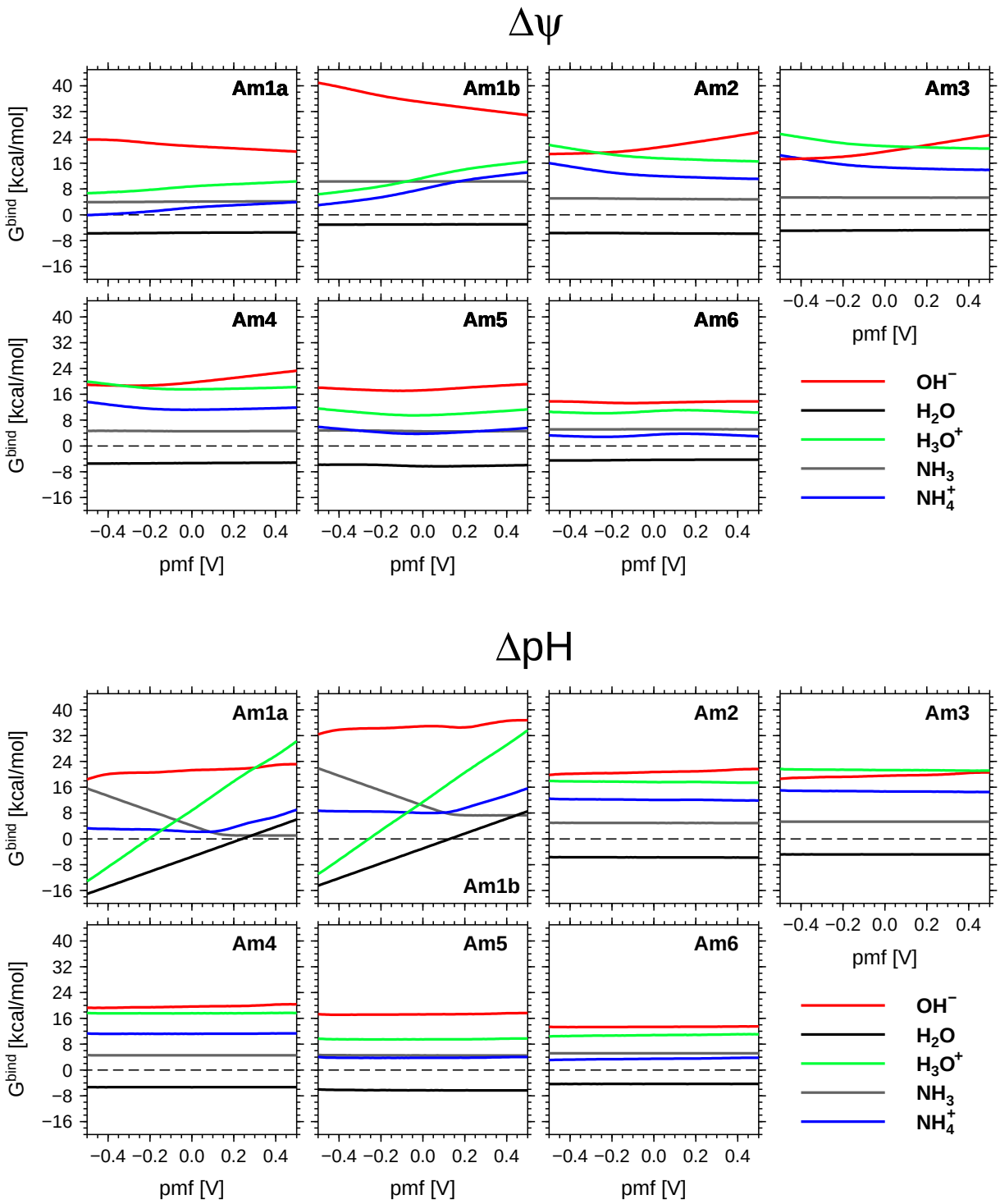

Figure S25: Binding free energy for different permeants at the transmembrane pore sites as functions of a proton-motive force. upper block: pmf consists entirely of an electric transmembrane potential. The pH is set to 7.0 on both membrane sides. lower block: pmf consists entirely of a transmembrane pH difference, The intracellular pH is set to 7.0. The extracellular pH is given by $7.0 + \mathrm{pmf}/59$ mV. For both blocks, the pN is set to 3.0 on both membrane sides.

G Free energy schemes with all considered transmembrane pore states

This section contains plots of the relative free energies of all states of the pore sites considered in deducing the possible transport mechanisms in the main text. The pH value is set to 7.0 on both membrane sides. The pN value is set to 3.0 on both membrane sides. Fig. S26 and Fig. S27 show the relative free energies of the states at a transmembrane potential of −120 mV. Fig. S28 and Fig. S29 show the corresponding plots at a transmembrane potential of 0 mV.

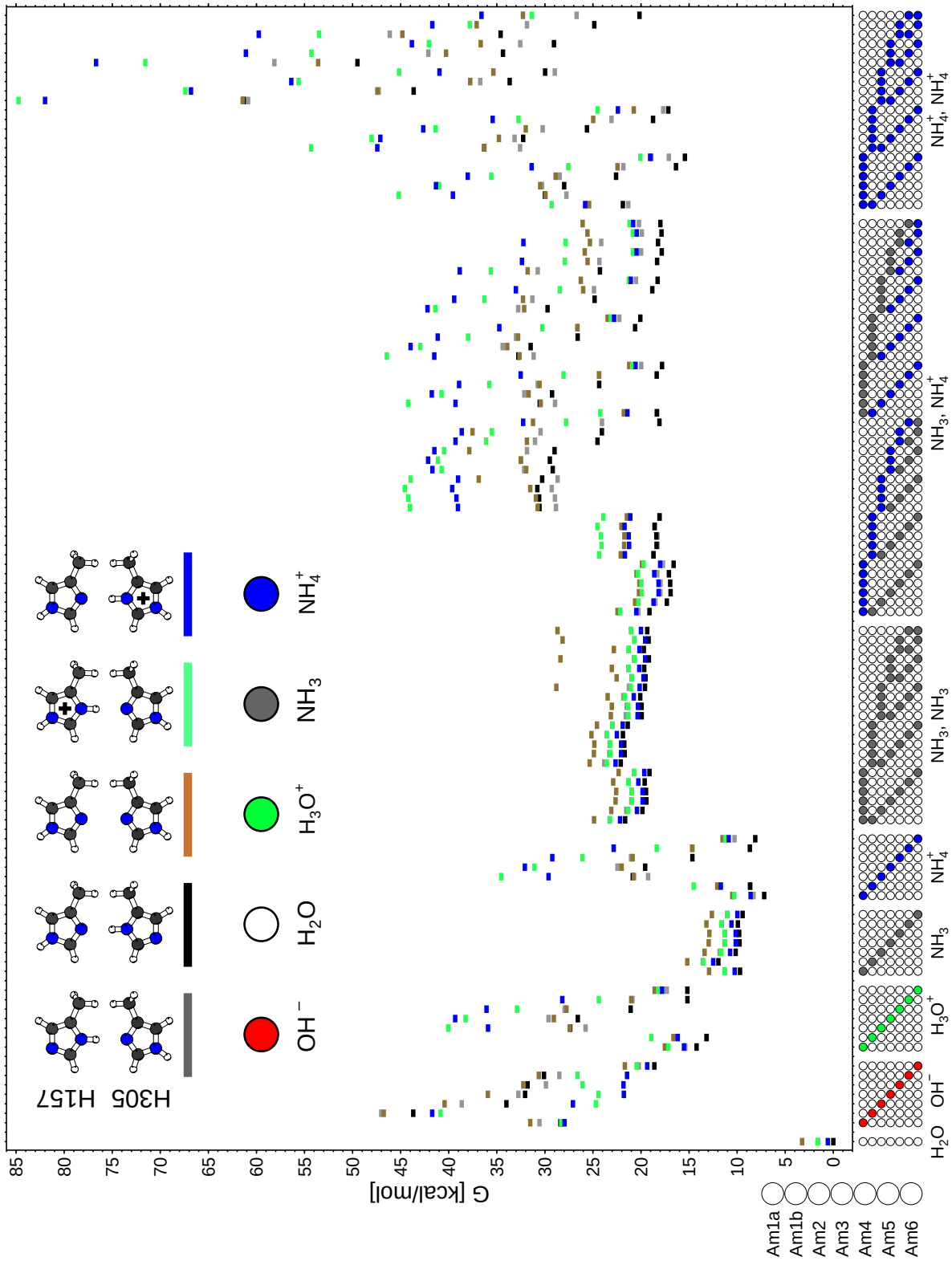

Figure S26: Energy level scheme for states of the permeant sites and the twin-His motif (pH = 7.0 and pN = 3.0 on both membrane sides, $\Delta\psi$ = -120 mV). The free energy of each state is plotted relative to the free energy of the fully water bound state with H157 adopting the Nϵ-protonated tautomer and H305 adopting the Nδ-protonated tautomer. The energy levels are color coded according to the configuration adopted by the twin-His motif as defined by the legend at the top of the scheme. The species present at the permeant sites (Am1a to Am6) are indicated at the horizontal axis: grey: NH_3, blue: NH_4^+, white H_2O, red OH^-, green H_3O^+.

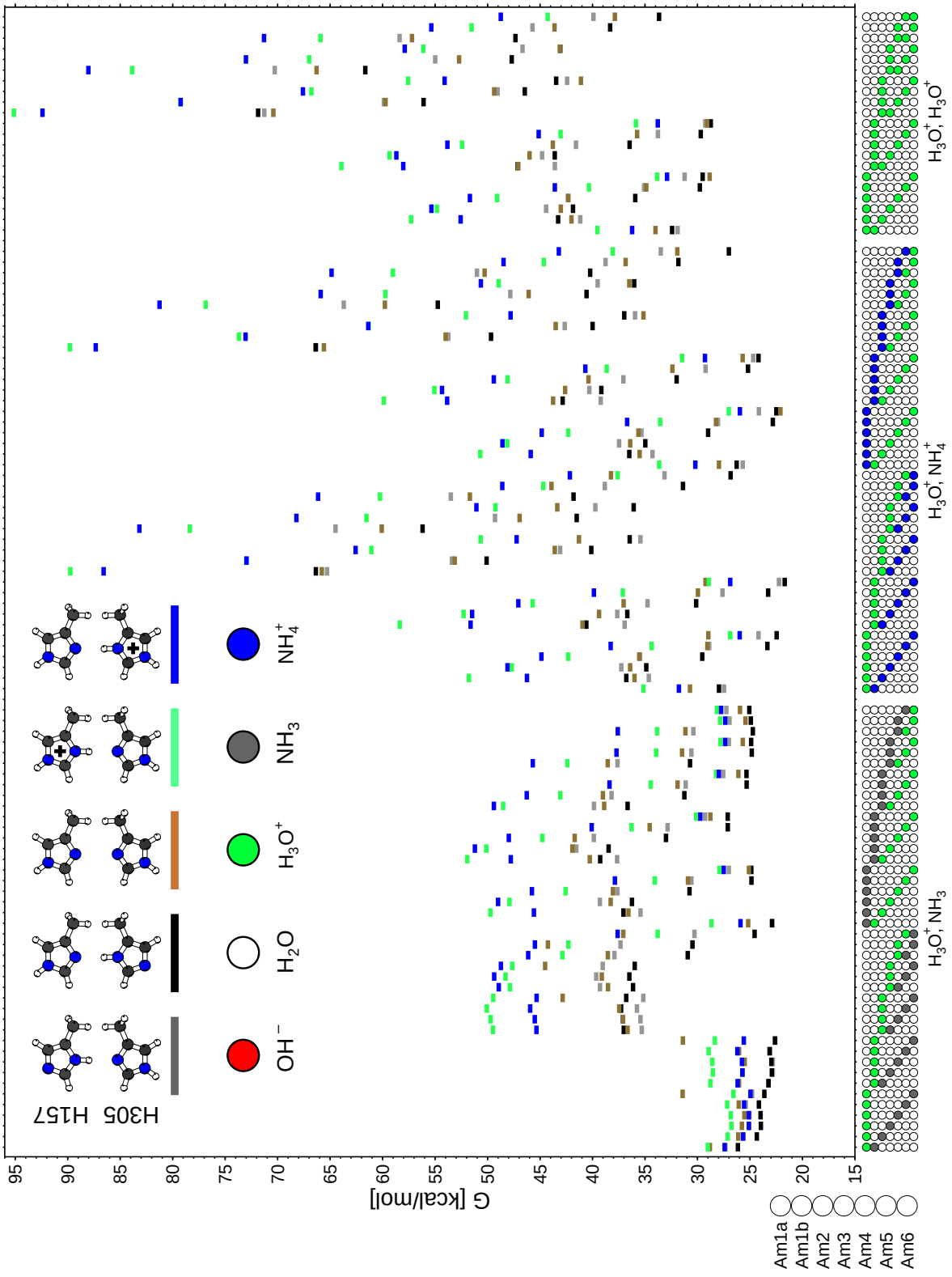

Figure S27: Continued from Fig. S26. Energy level scheme for states of the permeant sites and the twin-His motif (pH = 7.0 and pN = 3.0 on both membrane sides, $\Delta\psi$ = -120 mV). The free energy of each state is plotted relative to the free energy of the fully water bound state with H157 adopting the Nϵ-protonated tautomer and H305 adopting the Nδ-protonated tautomer. The energy levels are color coded according to the configuration adopted by the twin-His motif as defined by the legend at the top of the scheme. The species present at the permeant sites (Am1a to Am6) are indicated at the horizontal axis: grey: NH_3, blue: NH_4^+, white H_2O, red OH^-, green H_3O^+.

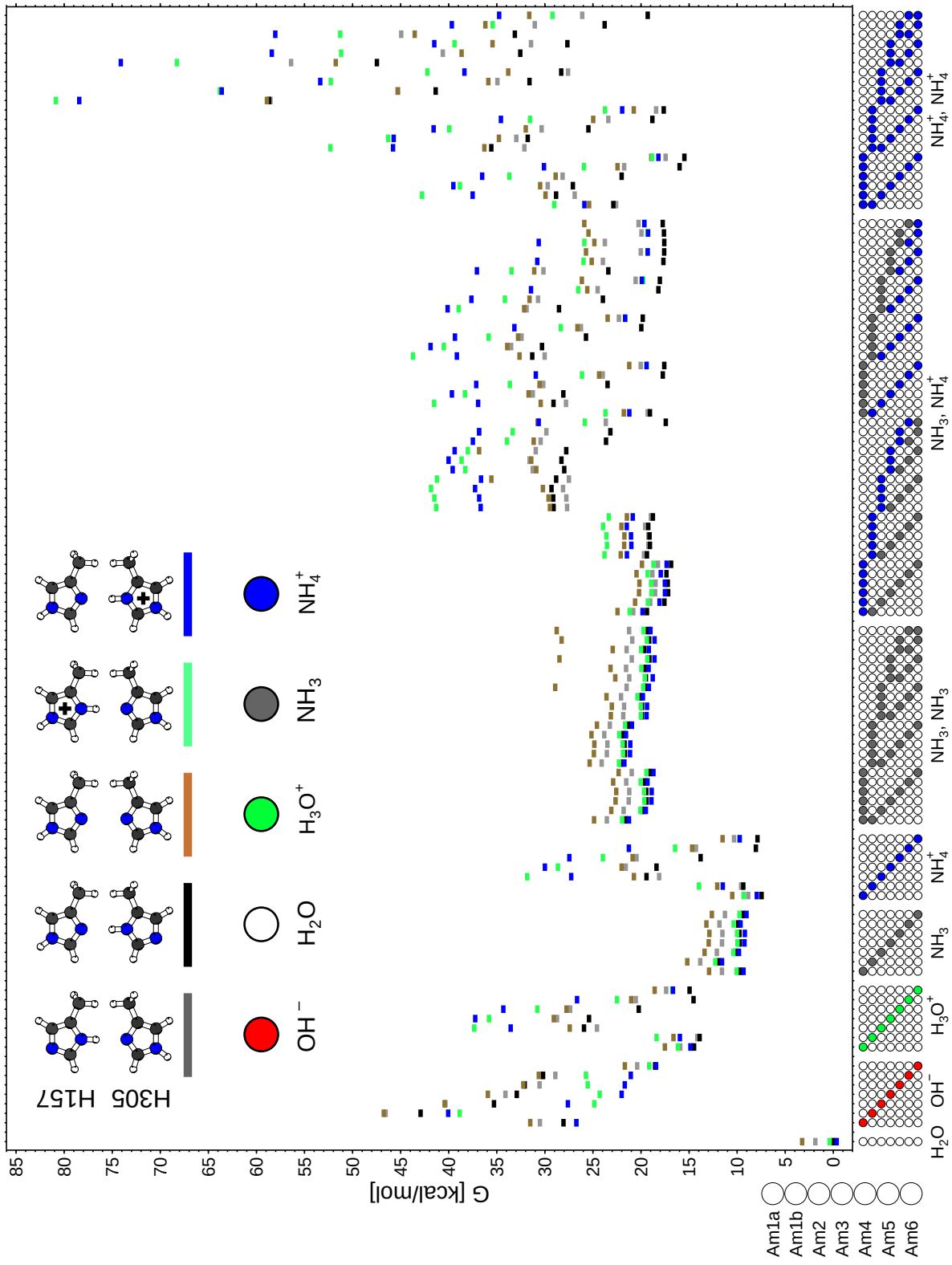

Figure S28: Energy level scheme for states of the permeant sites and the twin-His motif (pH = 7.0 and pN = 3.0 on both membrane sides, $\Delta\psi = 0$ mV). The free energy of each state is plotted relative to the free energy of the fully water bound state with H157 adopting the Nϵ-protonated tautomer and H305 adopting the Nδ-protonated tautomer. The energy levels are color coded according to the configuration adopted by the twin-His motif as defined by the legend at the top of the scheme. The species present at the permeant sites (Am1a to Am6) are indicated at the horizontal axis: grey: NH_3, blue: NH_4^+, white H_2O, red OH^-, green H_3O^+.

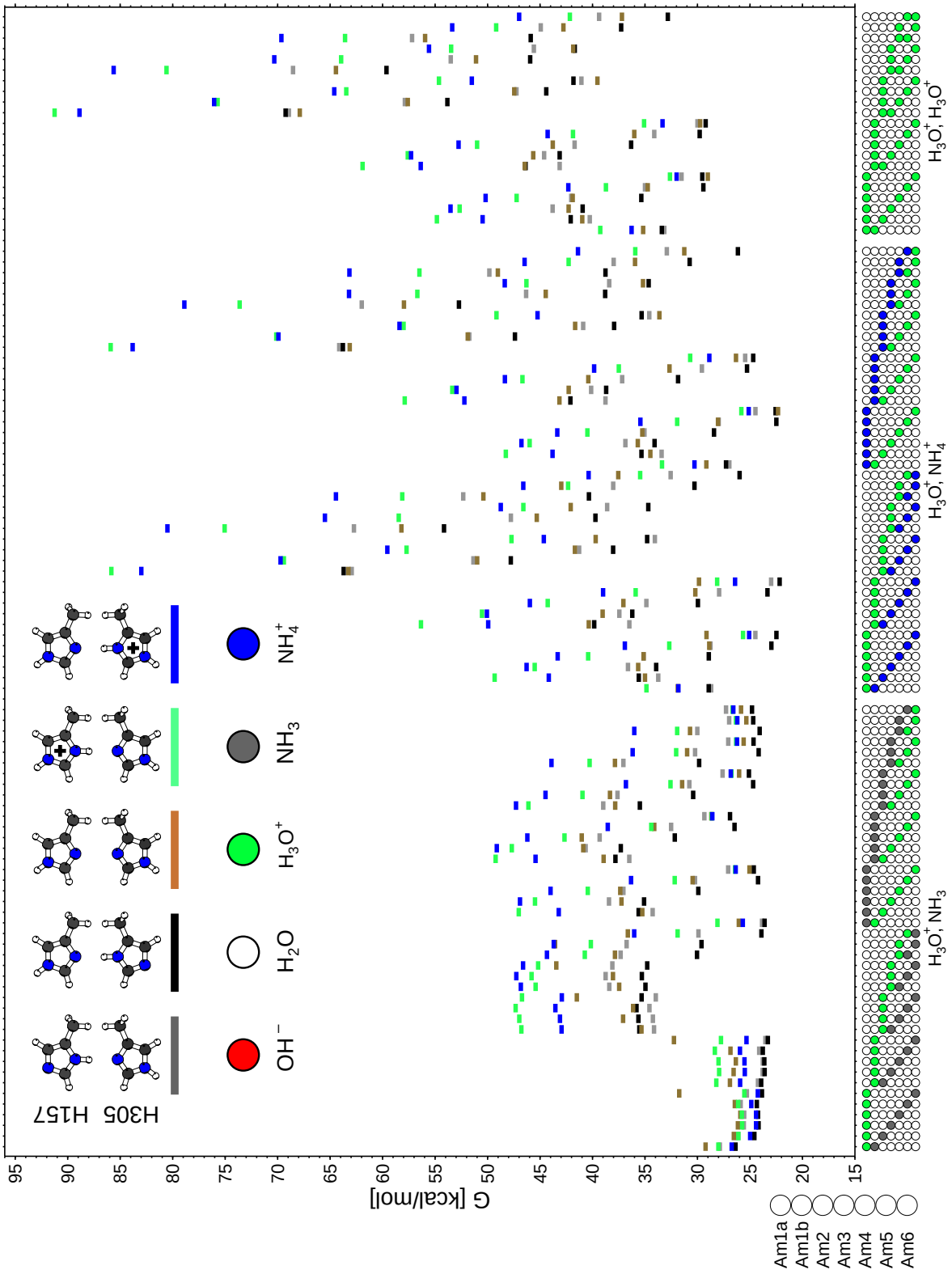

Figure S29: Continued from Fig. S28. Energy level scheme for states of the permeant sites and the twin-His motif (pH = 7.0 and pN = 3.0 on both membrane sides, $\Delta\psi = 0$ mV). The free energy of each state is plotted relative to the free energy of the fully water bound state with H157 adopting the Nϵ-protonated tautomer and H305 adopting the Nδ-protonated tautomer. The energy levels are color coded according to the configuration adopted by the twin-His motif as defined by the legend at the top of the scheme. The species present at the permeant sites (Am1a to Am6) are indicated at the horizontal axis: grey: NH_3, blue: NH_4^+, white H_2O, red OH^-, green H_3O^+.

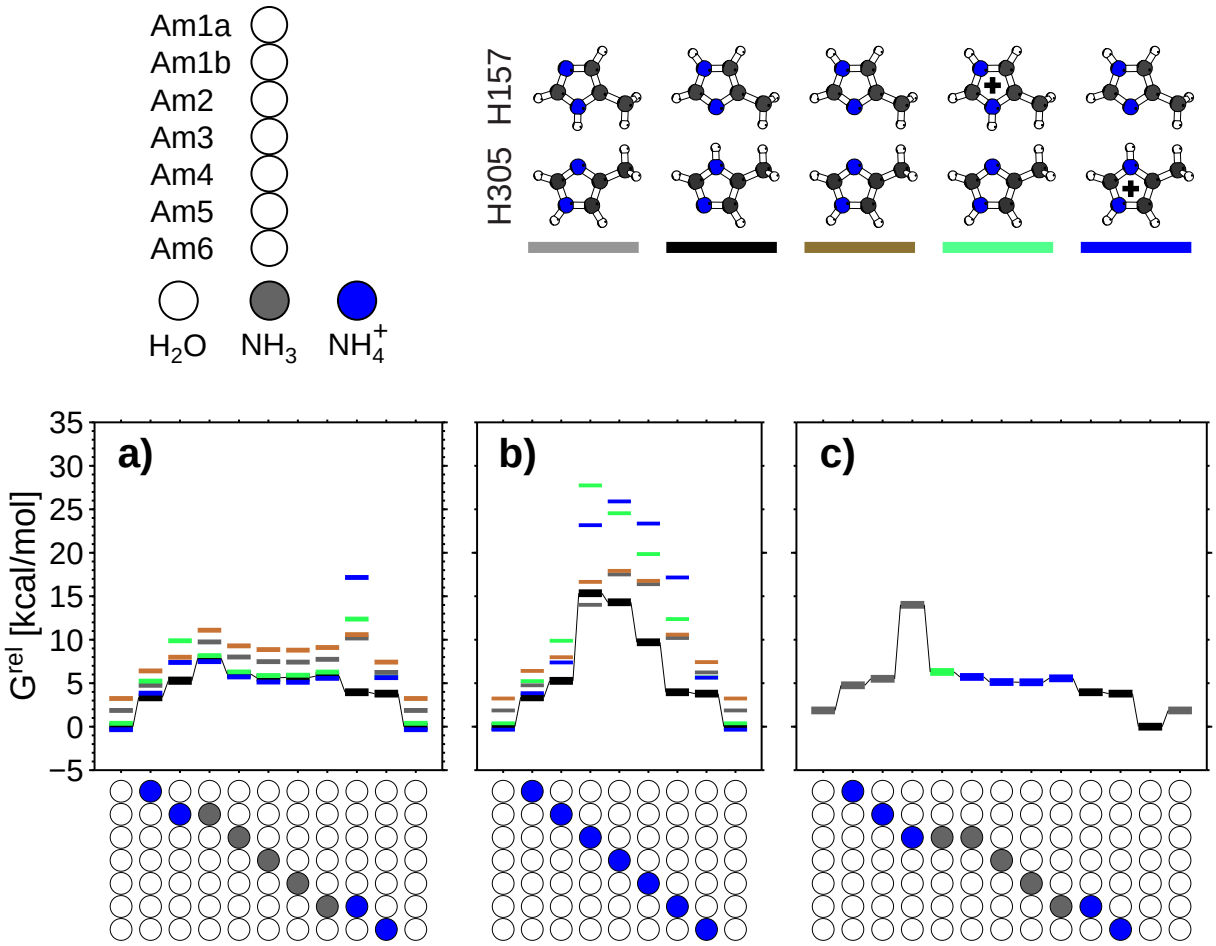

Figure S30: Free energy level scheme for states of the permeant sites and the twin-His motif occurring during different proposals for the permeation mechanism. This figure is similar to Fig. 7 of the main paper, but here we assume a a total concentration of 1 M for ammonia/ammonium and set all electrochemical transmembrane gradients to zero. Comparison to Fig. 7 of the main paper shows the effect of accounting for physiologically relevant values of the permeant concentrations and the electrochemical transmembrane gradients. The species present at the permeant sites (Am1a to Am6) are indicated at the horizontal axis (grey: NH_3, blue: NH_4^+, white: H_2O). The free energy of each state is plotted relative to the free energy of the state with all permeant sites occupied by water, H157 adopting the Nϵ-protonated tautomer and H305 adopting the Nδ-protonated tautomer. The energy levels are color coded according to the configuration adopted by the twin-His motif as defined by the legend. Connecting lines between the free energy levels are just a guide to the eye and do not imply transition state energies. The pH is set to 7.0 on both membrane sides. The pN is set to 0.0 on both membrane sides. $\Delta\psi$ is set to 0 V. **a)** electroneutral NH_3 uniport. **b)** electrogenic NH_4^+ uniport not involving protonation state changes of the twin-His motif. **c)** electrogenic NH_3/H^+ symport involving protonation state changes of the twin-His motif. It is not clear how the restoration of the twin-His motif's configuration between the last two stages of this mechanistic scheme will occur microscopically. The restoration might involve a transient reprotonation of the twin-His motif, proton transfer along the water molecules in the pore lumen and/or a transient reorientation of the histidine side chains.

References

[1] MacKerell, A. D; Bashford, D; Bellott, M; Dunbrack, R. L; Evanseck, J. D; Field, M. J; Fischer, S; Gao, J; Guo, H; Ha, S; Joseph-McCarthy, D; Kuchnir, L; Kuczera, K; Lau, F. T. K; Mattos, C; Michnick, S; Ngo, T; Nguyen, D. T; Prodhom, B; Reiher, W. E; Roux, B; Schlenkrich, M; Smith, J. C; Stote, R; Straub, J; Watanabe, M; Wiorkiewicz-Kuczera, J; Yin, D ; Karplus, M. *J. Phys. Chem. B* **1998**, *102*, 3586–3616.

[2] Ullmann, R. T; Ullmann, G. M. *J. Phys. Chem. B* **2011**, *115*, 10346–10359.

[3] Lopez, X; Schaefer, M; Dejaegere, A ; Karplus, M. *J. Am. Chem. Soc.* **2002**, *124*, 5010–5018.

[4] Ullmann, R. T; Ullmann, G. M. *J. Comput. Chem.* **2012**, *33*, 887–900.

[5] Tari, L. W. **2012** in *Structure-Based Drug Discovery*, Methods in Molecular Biology, ed. Tari, L. W. (Humana Press) Vol. 841, pp. 251–266.

[6] Cabini, S; Gianni, P; Mollica, V ; Lepori, L. *J. Solution Chem.* **1981**, *10*, 563–595.

[7] Wolfenden, R; Andersson, L; Cullis, P. M ; Southgate, C. C. B. *Biochemistry* **1981**, *20*, 849–855.

[8] Villa, A; Mark, A. E. *J. Comput. Chem.* **2002**, *23*, 548–553.

[9] Shirts, M. R; Pitera, J. W; Swope, W. C ; Pande, V. S. *J. Chem. Phys.* **2003**, *119*, 5740–5761.

[10] Mobley, D. L; Bayley, C. I; Cooper, M. D; Shirts, M. R ; Dill, K. A. *J. Chem. Theory Comp.* **2009**, *5*, 350–358.

[11] Till, M. S; Essigke, T; Becker, T ; Ullmann, G. M. *J. Phys. Chem. B* **2008**, *112*, 13401–13410.

[12] Debye, P; Hückel, E. *Phys. Z.* **1923**, *24*, 185–206.

[13] Tissue, B. M. **2012** *Basics of Analytical Chemistry and Chemical Equilibria.* (John Wiley & Sons Ltd.), 1st edition.

[14] Kielland, J. *J. Am. Chem. Soc.* **1937**, *59*, 1675–1678.

[15] Sörensen, S. P. L. *Biochem. Z.* **1909**, *21*, 131–200.

[16] Wiberg, E. **1972** *Die chemische Affinität.* (de Gruyter, Berlin/New York), 2nd edition.

[17] CRC Handbook of Physics and Chemistry. **1986** *(Weast, R. C. (Ed.)).* (CRC Press, Boca Raton, FL).

[18] Azzone, G; Benz, R; Bertl, A; Colombini, M; Crofts, A; Dilley, R; Dimroth, P; Dutton, P; Felle, H; Harold, F; Junge, W; Kaback, H; Knaff, D; Krulwich, T; Lodish, H; Malmström, B; Maloney, P; Mannella, C; Padan, E; Papa, S; Rottenberg, H; Rudnick, G; Rydström, J; Silverstein, T; Skulachev, V; Slayman, C; Tedeschi, H; Wikström, M ; Wilson, T. H. *BBA-Bioenergetics* **1993**, *1183*, 1–3.

[19] Roux, B. *Biophys. J.* **1997**, *73*, 2980–2989.